



**ST. ANTHONY MINE: PIT 1 HIGHWALL  
STABILITY – PHASE 2 REPORT**

29 August 2023

Prepared for:  
United Nuclear Corporation

Prepared by:  
Stantec Consulting Service Inc.

Project Number: 233001363

This document entitled ST. ANTHONY MINE PIT 1 HIGHWALL STABILITY - PHASE 2 REPORT was prepared by Stantec Consulting Services Inc. ("Stantec") for the account of United Nuclear Corporation (the "Client"). Any reliance on this document by a third party outside of its intended scope and conclusions is at the risk of the third party and the Client. The material in it reflects Stantec's professional judgment in light of the scope, schedule and other limitations stated in the document and in the contract between Stantec and the Client. The assertions in the document are based on conditions and information existing at the time the document was published and do not take into account any subsequent changes. In preparing the document, Stantec did not verify information supplied to it by others. Any use which a third party makes of this document is the responsibility of such third party. Such third party agrees that Stantec shall not be responsible for costs or damages of any kind, if any, suffered by it or any other third party as a result of decisions made or actions taken based on this document.

## Table of Contents

EXECUTIVE SUMMARY .....	IV
ACRONYMS / ABBREVIATIONS .....	VIII
1.0 INTRODUCTION.....	1
1.1 Background.....	1
1.2 Purpose.....	3
2.0 SITE DESCRIPTION.....	5
2.1 Site Location and Features.....	5
2.2 Regional Geology.....	5
2.3 Site Seismicity.....	6
3.0 GEOTECHNICAL FIELD INVESTIGATION.....	8
3.1 Geotechnical Borehole Drilling.....	9
3.2 Acoustic and Optical Televiewer Surveys.....	10
3.3 Dilatometer Testing.....	10
3.4 Core Sample Activity Screening.....	11
4.0 GEOTECHNICAL LABORATORY TESTING.....	12
4.1 Soil Sample Index Testing.....	12
4.2 Point Load Index Testing of Rock Core Samples.....	12
4.3 Unconfined Compressive Strength (UCS) of Rock Core Samples.....	13
4.4 Triaxial Compressive Strength of Rock Core Samples.....	14
4.5 Direct Shear Strength of Rock Core Samples.....	14
4.6 Durability Testing of Rock Core Samples.....	14
5.0 SUMMARY OF SUBSURFACE CONDITIONS.....	15
5.1 Overburden.....	15
5.2 Bedrock.....	15
5.2.1 Total Core Recovery, Solid Core Recovery and Rock Quality Designation.....	16
5.2.2 Geological Strength Index (GSI).....	18
5.2.3 Unconfined Compressive Strength.....	19
5.2.4 Discontinuities.....	20
5.2.5 Discontinuity Strength.....	24
5.3 Groundwater Condition.....	25
5.4 Core Sample Activity Measurements.....	26
6.0 SLOPE STABILITY ANALYSIS.....	27
6.1 Kinematic Analysis.....	27
6.2 Results of Kinematic Analysis.....	28
6.3 Potential Instabilities Involving Major Structures.....	29
6.4 Slope Stability Analysis.....	30
6.5 Methodology.....	32
6.5.1 Slope Parameters.....	32
6.5.2 Rock Parameters.....	32
6.5.3 Groundwater.....	34
6.5.4 Seismic Parameters.....	34



6.5.5	Geometric Search Constraints.....	34
6.6	Stability Analysis Results.....	35
6.6.1	Static Stability.....	35
6.6.2	Pseudo-static.....	36
6.6.3	Shallow Static Stability.....	37
7.0	ROCKFALL ANALYSIS.....	39
7.1	Methodology.....	40
7.2	Rockfall Parameters.....	40
7.3	Slope Parameters.....	41
7.3.1	Modified Pit Slope Alternatives.....	43
7.4	Results.....	44
7.4.1	Modified Pit Slope – Partial Backfill.....	47
7.4.2	Modified Pit Slope – Berms, Backfill, and Benches.....	47
7.5	Discussion.....	48
7.5.1	Existing State – Critical Risks.....	48
7.5.2	Improved State – Mitigation Strategy.....	49
8.0	CONCLUSIONS AND RECOMMENDATIONS.....	51
8.1	Slope Stability.....	51
8.2	Rockfall Hazards.....	51
8.3	Recommended Next Steps.....	52
9.0	REFERENCES.....	53

**List of Tables**

Table 1:	Borehole Details.....	10
Table 2:	Soil Sample Index Test Results.....	12
Table 3:	Triaxial Compressive Strength Test Results.....	14
Table 4:	Bedrock Stratigraphy.....	16
Table 5:	TCR and RQD.....	17
Table 6:	Geological Strength Index (GSI) values.....	18
Table 7:	Unconfined Compressive Strength (UCS) Test Results.....	20
Table 8:	Discontinuity Input Parameters.....	25
Table 9:	Results of the Kinematic Analysis for All Discontinuities.....	28
Table 10:	Results of Kinematic Analysis for Discontinuities in Joint Sets.....	28
Table 11:	Hoek-Brown Average Material Parameters.....	33
Table 12:	Lower Bound Hoek-Brown Parameters.....	33
Table 13:	Global Static FOS Results.....	35
Table 14:	Global Pseudo-Static FOS Results.....	37
Table 15:	Surficial Static FOS Results.....	37
Table 16:	Rockfall Model Input Parameters.....	41
Table 17:	Rockfall Analysis – Input Parameters Slope Material.....	42
Table 18:	Summary of Rockfall Analysis Results.....	44



## List of Figures

Figure 1:	Pit Wall Locations.....	3
Figure 2:	Site Location .....	5
Figure 3:	Hazard Curves from USGS Unified Hazard Tool for the PGA.....	7
Figure 4:	Borehole Location Diagram .....	8
Figure 5:	ShapeMetrix3D Model .....	21
Figure 6:	Stereographic Plot with All Discontinuities.....	22
Figure 7:	Symbolic Stereographic Plot with All Discontinuities.....	22
Figure 8:	Bedding Discontinuity Orientation Summary .....	23
Figure 9:	Joint Sets Discontinuity Orientation Summary.....	24
Figure 10:	Pit 1 Highwall Stability and Rockfall Sections.....	31
Figure 11:	SS-4 with Weak Zones Showing all Non-Circular Surfaces with FOS < 2 .....	36
Figure 12:	Example of Slope Model – Section 4 (Calibration Run).....	43
Figure 13:	Simulated Rockfall Bench Cleaning Locations .....	48
Figure 14:	Conceptual Berm Placement .....	50

## Appendices

Appendix A	Phase 2 Workplan.....	A-1
Appendix B	Site Plan .....	B-1
Appendix C	Borehole Logs .....	C-1
Appendix D	Photologs .....	D-1
Appendix E	Data Visualization .....	E-1
Appendix F	Televiwer Logs .....	F-1
Appendix G	Dilatometer Results.....	G-1
Appendix H	Radiation Scan Data .....	H-1
Appendix I	Lab Test Results .....	I-1
Appendix J	GSI .....	J-1
Appendix K	Kinematic Results .....	K-1
Appendix L	Slope Stability Results .....	L-1
Appendix M	Rockfall Results .....	M-1



## EXECUTIVE SUMMARY

This report describes the Phase 2 borehole investigation and detailed rockfall and slope stability modeling program. Stantec completed a Phase 1 preliminary slope stability assessment and gap analysis of the St. Anthony Pit 1 Highwall in 2021. A subsurface borehole investigation and laboratory testing program was conducted to better define the highwall bedrock stratigraphy and bedrock properties assumed for Phase 1. Information from the subsurface investigation was used to verify the rock strengths in the profile for the slope stability model in order to justify adequate long-term factor of safety (FOS) for the highwalls of Pit 1. Consistent with the 30% Closure Closeout Plan (CCOP) prepared by Stantec for the St. Anthony mine (Stantec, 2022), Pit 1 will be partially backfilled and up to approximately 255 feet of the pit high walls will remain. The highwall from top to bottom consists of Mancos Shale and Sandstone, Dakota Sandstone, and the uranium ore-bearing Jackpile formation.

A rock fall modeling program was used to delineate hazard zones and effectively design hazard avoidance, evaluate hazard protection solutions. The model simulated rock falls from various locations and heights along the highwall and calculated the trajectories and impact forces expected. This included calibration modeling to review current conditions as well as forward (prediction) modeling for the current slope trajectory and for changes to the trajectory once the benches accumulate additional scree. The results of the rock fall modeling will allow for design of rockfall mitigation measures in the pit bottom to be incorporated with the proposed design for the Pit 1 reclamation.

The Site is located in Cibola County, New Mexico, in a remote, sparsely populated area of the Cebolleta Land Grant approximately 40 miles west of Albuquerque and 4.6 miles southeast of Seboyeta. UNC operated the St. Anthony Mine, comprised of an open pit and underground shaft uranium mine, from 1975 to 1981.

### Investigation

The geotechnical field investigation took place over the period of 10 November 2021, to 28 January 2022. Five boreholes were drilled under the supervision of Stantec personnel. Subsurface conditions were logged in the field by Stantec geologists and/or geotechnical engineers. Two boreholes were drilled at an incline of approximately 25 degrees from vertical.

The boreholes were advanced with the use of an Acker Renegade track mounted drill rig equipped for geotechnical sampling and testing. Standard penetration tests (SPT) were conducted at 5-foot intervals within the overburden soils, using a 2.5-inch outside diameter (od) split spoon (SS) sampler. Bedrock was cored with oversize NQ and HQ diamond drill bits using a triple inner tube system to recover the rock core samples.

The Total Core Recovery (TCR), Solid Core Recovery (SCR) and Rock Quality Designation (RQD), were measured and recorded by Stantec. Core samples were screened for radiation. Detailed rock core run logging was completed in the inner sleeve of the triple tube sampler.



Overburden samples selected for classification and index property testing and Core samples selected for strength testing were packaged carefully and transported to Advanced Terra Testing (ATT) for laboratory testing.

Dilatometer testing was completed in borehole BH-3 and acoustic and optical televiewer surveys were completed in the two inclined boreholes. The dilatometer testing and televiewer surveys were completed by COLOG.

### **Slope Stability Analysis**

#### *Kinematic analysis*

A kinematic analysis was performed to evaluate the potential for structurally controlled slope failures using the structural information gathered from the site investigation. The kinematic analysis was carried out using the software Dips 8.0 from Rocscience to evaluate the potential for planar, wedge, and toppling failure modes using stereographic projections.

The orientations (dip and dip direction) of the discontinuities encountered in the boreholes were identified from the televiewer data collected in each borehole and from the ShapeMetrix<sup>3D</sup> model which collected data from a drone survey of the highwalls. The discontinuities in the rock mass are dominated by the sub-horizontal bedding of the sedimentary rock formations. A smaller subset of discontinuities, identified as J<sub>1</sub>, have a mean dip of 87 degrees  $\pm$  20 degrees dipping toward to the west and partly overturned toward the east. The oriented data was plotted on a stereonet for visualization and interpretation.

The sub-horizontal major discontinuity set (bedding) observed in the boreholes and ShapeMetrix 3D data does not support kinematic sliding failures along the discontinuities, such as planar and wedge sliding failures. There is kinematic potential for planar failures in sets J<sub>2</sub> and J<sub>3</sub> along the west and north highwalls, respectively, and toppling failures in set J<sub>1</sub> on the west highwall. Although the kinematic results show that these discontinuity sets are oriented in potential failure planes, this does not indicate a likelihood of failure. A majority of the televiewer discontinuities in these sets were healed and would provide greater frictional resistance against failure. Planar failure would require daylighting of the noted joint sets along the top of the highwall which was not observed in the joint set data or visually in the field. Toppling failure is unlikely for discontinuities in set J<sub>1</sub> due to their steepness and intermittent nature.

#### *Slope Stability analysis*

The slope stability analysis was completed using industry standard methods following general guidance from Guidelines for Open Pit Slope Design (Read and Stacey, 2019) and Rock Slope Engineering (Wyllie, 2018). Five sections along the pit highwall were used for the slope stability analysis. Sections were chosen based on borehole locations with an additional section chosen between boreholes, along the northeast highwall (Section 1.0).

All rock formations except the Mancos Shale were modeled using Hoek-Brown Generalized failure criterion assuming the rock mass shear strength is generally isotropic. The Mancos Shale



was modeled assuming anisotropic rock mass characteristics. The analysis has assumed a uniform blast damage zone depth of approximately 45 ft (1.5 times the estimated bench height) from the existing pit slope face into the rock mass. A blast damage factor of  $D = 1.0$  (Hoek, 2000) was applied to the Hoek Brown material properties.

Limit equilibrium analysis was carried out using the software Slide2 from Rocscience Inc. (Rocscience, 2020). The analysis considered both circular and non-circular failure types. Slopes were analyzed for both shallow failures along the surface, or failure of a single bench, and global failures along planes deeper into the highwall through multiple benches. Static and pseudo static loading conditions were analyzed.

The selected minimum FOS values for comparison used for these analyses are 1.3 for static, 1.0 for pseudo static conditions, and 1.1 for shallow bench-scale failure based on criteria for a low consequence of failure pit (Read, 2019 [Table 9.9]). These FOS were used as general guidance for the analyses and comparison with the calculated values. Pit 1 was assigned a low consequence of failure because it is a closed pit located on remote private land that will have restricted access upon completion of reclamation as described in the 30% CCOP (Stantec, 2022). The stability model scenarios met the minimum comparison factors of safety. The 45 ft blast damage zone generally controlled failure surfaces. Small scale, surficial failures generally had the lowest factors of safety.

In general, stability results indicate global and surficial stability of the highwall. For these conditions, large scale slope cuts are not recommended. Surficial scaling of the highwall is recommended, based on visual observations, to mitigate for rockfall and potential surficial failures at a smaller scale than captured in the model. A majority of the scaled materials are expected to be the Mancos and Dakota bedrock. Surficial scaling of the pit walls and placement of materials in the pit would not impact global stability results.

### **Rockfall Analysis**

The rockfall analysis conducted in Phase 2 was undertaken using the program Rocfall version 6.0 from Rocscience (Rocscience, 2018), which is part of the same software suite as the stability analysis completed for the pit. The Rigid Body Method analysis was chosen to take into account site specific rockfall variables from observations made within the pit and to allow modelling of different particle shapes and sizes. The Rigid Body Method applies impact mechanics to rockfall, is common practice in industry, and considers the impact of an initially hard rigid body (rock block) with the slope considered as a short stiff spring (Wylie, 2015).

The supplemental rockfall analysis for Phase 2 was undertaken using 8 sections (RF-1 through RF-8) distributed around the Pit 1 highwall. All sections were run in their existing state, and sections RF-4 through RF-7 were also ran with preliminary conceptual pit backfill and 2-meter waste rock berm designs for comparison.



During the Phase 1 analysis, Stantec collected field observation data through photographs and manual measurements of detached rock blocks found on the pit floor and observed on the highwalls. These measurements and observations were used to inform our modelling approach for rock sizing and shapes that occur at the site.

The slope materials used in the rockfall modelling to represent the pit surface were selected based on visual observations of slope features present during our Phase 1 assessment along with geological formations encountered during the 2021-22 drilling investigation at BH-1 through BH-4 around the pit highwall.

The results of the rockfall analysis for Pit 1 indicate great variability in rockfall retention, runouts, and potential bounce heights for all seeder locations considered per section. Rockfall retention varied from as little as 35% up to 99.9%, runouts beyond the toe-of-slope ranged from 18-feet to 105-feet, and bounce heights at strategic locations from the highwall toe range from 2-feet to over 20-feet. The highest energy encountered at a collector location was around  $9 \times 10^5$  ft-lbs from a mid-slope originating rock.

Rockfall model results indicate that non-ore bearing sandstone and siltstone formations on the west highwall presents the greatest rockfall hazard requiring mitigation methods as part of the closure plan. Stantec recommends the following actions and mitigation strategies:

- Mitigation options in the pit bottom involving a physical barrier to limit rockfall runout, which could include rock-filled barriers, a ditch, berm, or any combination of these options. Further modeling is required to verify sizing which will be included in the 90% CCOP.
- Scaling (removal of loose-hanging eroded rock blocks) and debris removal Dakota and Mancos formations along the pit crest, mid-slope benches, and the toe of the slope to decrease the immediate rockfall hazards.
- Rockfall signage and specific guidance on setback distance to be maintained during O&M activities should be implemented for both construction and closure. Details will be provided in the 90% CCOP.



## ACRONYMS / ABBREVIATIONS

AEP	Annual exceedance probability
ATT	Advanced Terra Testing
AVM	AVM Environmental Services
BH	borehole
CCOP	Closure Closeout Plan
DMP	Dilatometer Test
FOS	factor of safety
ft	feet
GISTM	Global Industry Standard on Tailings Management
GSI	Geological Strength Index
GLE	general limit equilibrium
GPS	global positioning system
ISRM	International Society for Rock Mechanics
JCON	joint condition rating
JCS	joint wall compression strength
JRC	joint roughness coefficient
kips	kilo pound
kPa	kilopascal
lb	pound
LIDAR	light detection and ranging
MMD	New Mexico Mining and Minerals Division
od	outside diameter
PGA	peak ground acceleration
PLT	point load test
psi	pound per square inch
RMR	rock mass rating
RQD	rock quality designation
SCR	solid core recovery
SPT	standard penetration test
SS	split spoon
TCR	total core recovery
USGS	United States Geological Survey
UCS	unconfined compressive strength
UNC	United Nuclear Corporation



## **1.0 INTRODUCTION**

On behalf of the United Nuclear Corporation (UNC), Stantec Consulting Services Inc (Stantec) completed a slope stability assessment and rockfall hazard analysis of the St. Anthony Mine Pit 1 Highwall to support preparation of the Closure-Closeout Plan (Stantec, 2022). The scope of work covered in this report is limited to investigation and analyses of the Pit 1 highwalls.

The pit walls are being evaluated to comply with NMAC 19.10.5.506, 507, and 508 as part of the non-coal mining regulations for existing Mining Operations Closeout Plans and Performance and Reclamation Standards and Requirements. The primary objective is to evaluate and reduce “current or future hazard to public health or safety” (NMAC 19.10.5.507.B.2) related to the open pit. Public access to the pit will be restricted as a part of the final closure design (Stantec, 2022), therefore, instability of the pit highwall and rockfall hazards would not impact public health or safety. The stability of the pit walls is being assessed to evaluate stable placement of the proposed surface water diversion structures west of the highwall, reduce potential for mass movement into the pit bottom, protect workers from rockfall hazards during closure construction, and develop a long-term design that controls erosion. Based on Guidelines for Open Pit Slope Design (Read, 2019 [Table 9.9]), Stantec selected a minimum factor of safety (FOS) of 1.3 for global long-term static conditions, 1.0 for pseudo-static conditions, and 1.1 for shallow bench failure for the Pit 1 Highwall as a low consequence of failure structure. Because of the competency of the lower rock strata, the Dakota and Jackpile formation, scaling, and removal of erosion debris from the highwall for stability and rockfall hazard reduction will focus on the upper Mancos Shale formation. Some materials may be scaled from the lower formations; however, these are expected to make up a small portion of the total volume.

This report presents the results from the field study and data analysis and provides recommendations for remedial measures.

### **1.1 Background**

The St. Anthony Mine was an open pit and underground shaft uranium mine located in a remote, sparsely populated area on the Cebolleta Land Grant approximately 40 miles west of Albuquerque and 4.6 miles southeast of Seboyeta. UNC operated the St. Anthony Mine from 1975 to 1981, pursuant to a mineral lease with the Cebolleta Land Grant, the current surface and mineral rights owner. The original lease covered approximately 2,560 acres. This lease was obtained on 10 February 1964, and was surrendered by a Release of Mineral Lease dated 24 October 1988. UNC has access to the Site with the permission of the Cebolleta Land Grant and Lobo Partners, LLC.

In January 2006 a Closeout Plan and a Materials Characterization Plan were submitted to the New Mexico Mining and Minerals Division (MMD) for the St. Anthony Mine Site (the Site) and a materials characterization program followed in 2006 and 2007. This program included drilling and



## **St. Anthony Mine: Pit 1 Highwall Stability – Phase 2 Report**

### **1.0 Introduction**

sampling on the existing waste piles. In 2018, supplemental investigations were carried out that included additional materials characterization and a geotechnical investigation with drilling on the waste piles, test pitting between piles, and characterization of borrow sources for the proposed design and construction. The 2006 Closeout Plan was then revised, updated, and submitted in March 2019 to the MMD. MMD provided comments on that plan requesting further evaluation of the Pit 1 highwalls and the potential inclusion of remedial safety measures to address wall stability. A revised CCOP for the Site was submitted in October 2022. Results of the Pit 1 highwall stability evaluation and any additional modeling results and design details will be incorporated into the 90% CCOP.

This investigation, as well as the Phase 1 preliminary highwall stability analysis completed in 2021, included in Appendix A, are intended to fill data gaps to address Pit 1 highwall stability questions and support the closeout design.

The Pit 1 highwalls at the Site have been separated, for the purposes of analyses, into four areas: 1) West Highwall, 2) South Highwall, 3) North Highwall, and 4) Northeast Highwall as shown in Figure 1. The Northeast Highwall is the shortest portion of the highwall and includes ramps descending to the bottom of the pit. This highwall is not critical for slope stability compared to the other highwalls on the north, south, and west sides of the pit. Therefore, a borehole was not drilled along this highwall and stratigraphy from the North Highwall adjusted based on bedrock slope trends from the other boreholes was used for the analyses completed on this highwall.



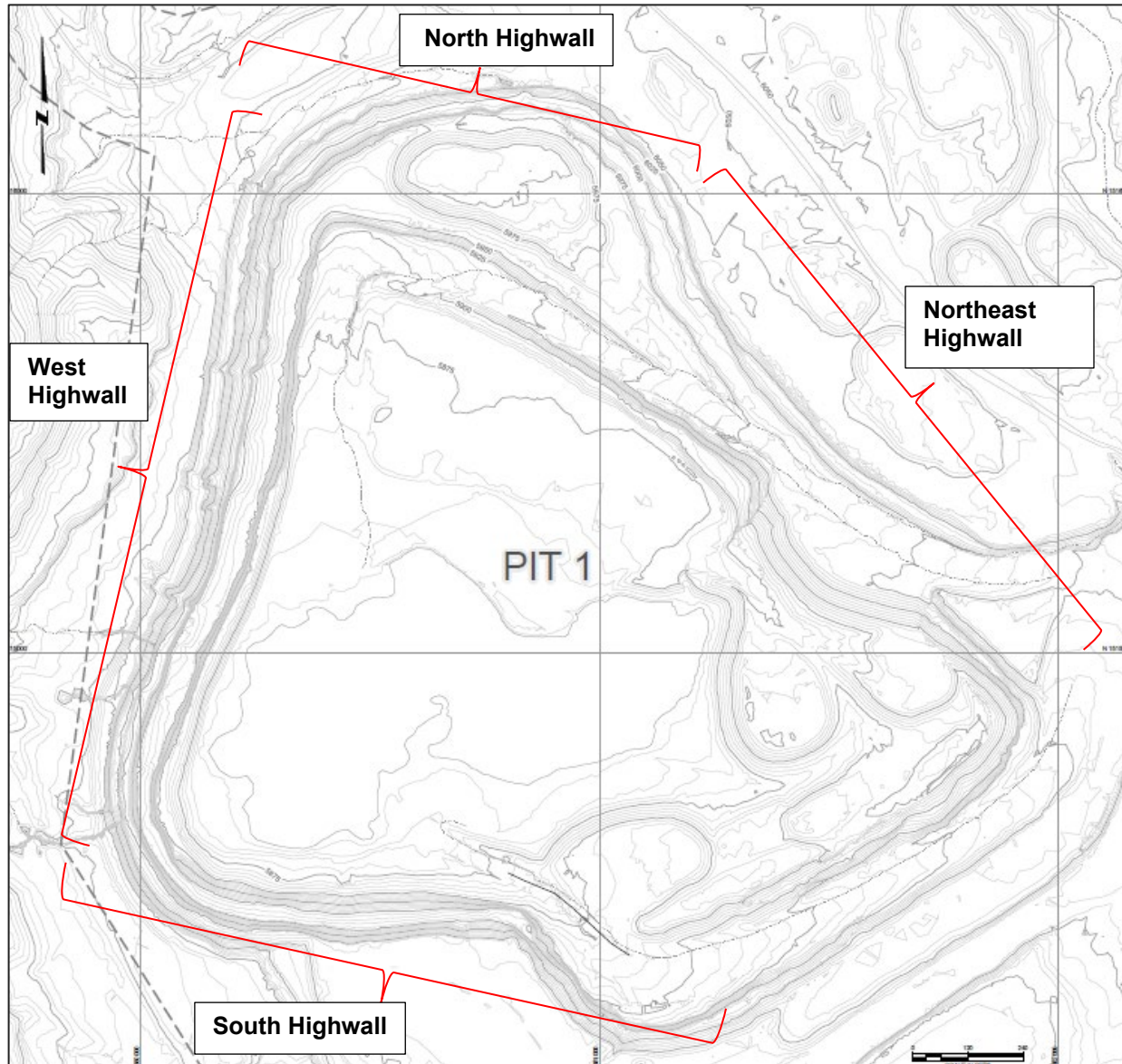


Figure 1: Pit Wall Locations

## 1.2 Purpose

This report describes the Phase 2 borehole investigation and detailed rockfall and slope stability modeling program. Stantec previously completed a Phase 1 preliminary slope stability assessment and gap analysis of the St. Anthony Pit 1 Highwall in 2021. The Phase 1 assessment identified gaps and a subsurface borehole investigation and laboratory testing program was conducted to better define the highwall bedrock stratigraphy and bedrock properties assumed for Phase 1. Information from the subsurface investigation was used to confirm the rock strengths adopted for the slope stability model to justify adequate long-term factor of safety (FOS) for the highwalls.



**St. Anthony Mine: Pit 1 Highwall Stability – Phase 2 Report**  
**1.0 Introduction**

Rock fall modeling was conducted to review hazard avoidance, or hazard protection solutions. The model simulated rock falls from various locations and heights along the highwall and calculated the rock fall trajectories and impact forces. This included calibration to current conditions as well as forward (prediction) modeling for the current slope trajectory and for changes to the trajectory once the benches accumulate additional scree during closure. The results of the rock fall modeling will allow for design of rockfall mitigation measures in the pit bottom to be incorporated into the 90% CCOP.



## 2.0 SITE DESCRIPTION

### 2.1 Site Location and Features

The mine site location is shown in Figure 2. The two open pits at the Site are in Sections 19 (Pit 1) and 30 (Pit 2), Township 11 North, Range 4 West, and the entrance to the underground mine is in Section 24, Township 11 North, Range 5 West. The Site includes underground workings comprising one mine shaft and several vent shafts that are now sealed at the surface, two open pits, numerous smaller piles of non-economical mine materials, and three topsoil and/or overburden piles. Under the proposed reclamation, Pit 1 would be partially backfilled and has three primary highwalls which are oriented generally towards east, south, and north. Other areas of Pit 1 contain expressed water, waste rock stockpiles, and access roads. The stability of the Pit 1 highwalls are evaluated in this report.

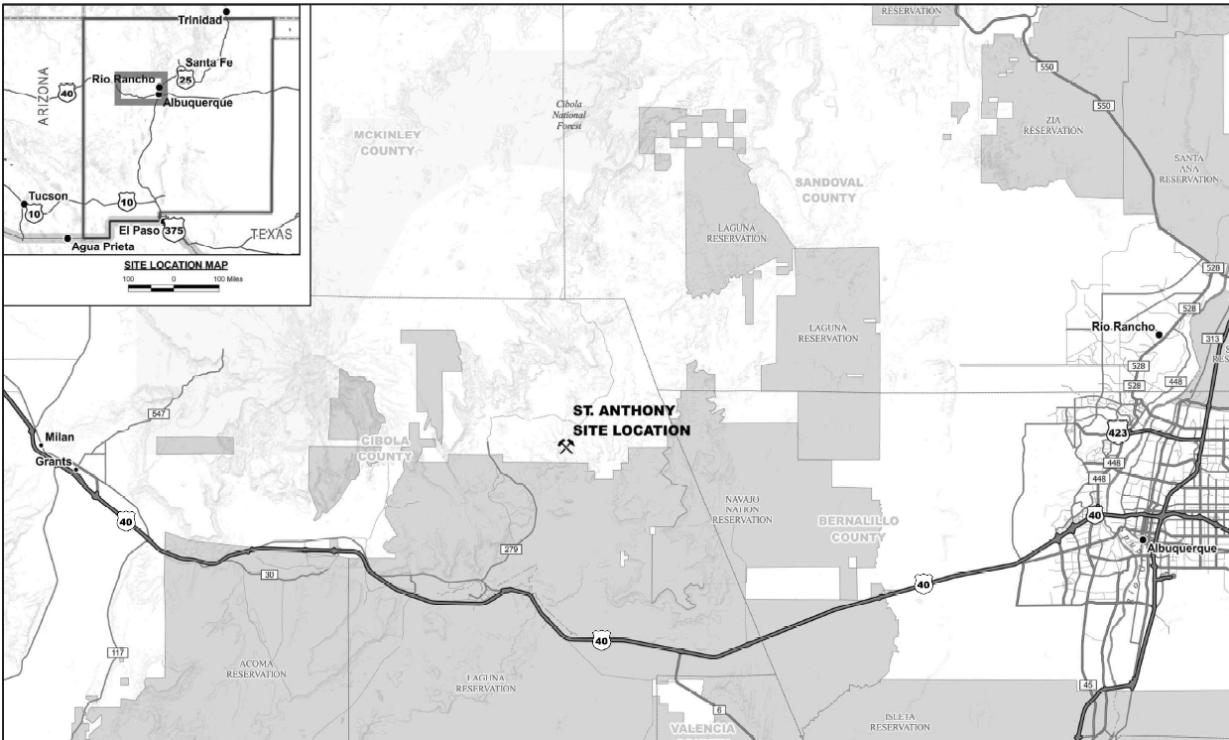


Figure 2: Site Location

### 2.2 Regional Geology

The Site is on the Colorado Plateau physiographic province, broadly characterized by plateaus and mesas of stratified sedimentary rock overlying tectonically stable Precambrian basement. Within the southeastern portion of the Colorado Plateau lies the San Juan Basin, a structural depression encompassing most of northwestern New Mexico and adjoining parts of Colorado and



## St. Anthony Mine: Pit 1 Highwall Stability – Phase 2 Report

### 2.0 Site Description

Utah. The strata of the San Juan Basin dip gently to the north (approximately 2 degrees), although small faults and folds alter the dip of the strata locally. The San Juan Basin is truncated on its southeastern margin by the Jemez lineament, a northeasterly trending structural boundary between the Colorado Plateau to the northwest and the Rio Grande Rift to the south and east. The Site is on the eastern edge of, and within, the Grants uranium district that lies on this transitional margin amidst many prominent Late Cenozoic volcanic fields that demarcate the Jemez lineament and the southeast margin of the San Juan Basin.

Sediments in the Grants area were deposited in various continental environments. During later Permian time, Glorieta sandstone and San Andreas limestone were deposited. The region was subsequently uplifted in Laramide time and the sediments of the Chinle Formation, San Rafael Group, and Morrison Formation were deposited. Upper Cretaceous strata consist of marine shore zone sandstones, marine shales, and various continental deposits. In ascending order, these are represented by the Dakota Sandstone, Mancos Shale, and the Mesaverde Group.

#### Site Geology

Stratigraphy of interest in the area of Pit 1 at the Site includes the Mancos Formation (Late Cretaceous), the Dakota Formation (Early and Late Cretaceous) and the Morrison Formation (Late Jurassic). The surficial geologic unit at Pit 1 is the Mancos Formation consisting of three sandstone units and interbedded shale units with a maximum thickness observed in the boreholes along the highwall of approximately 200 ft. The upper sandstone caps the Gavilan Mesa to the south of the pits. The Dakota Formation sandstone is located below the Mancos Formation and is 14 to 18 ft thick in the Pit 1 highwall boreholes. The Morrison Formation is approximately 600 ft thick and is below the Dakota Formation. The Morrison Formation is comprised of the Jackpile Member (sandstone), the Brushy Basin Member (interlayered mudstone and sandstone), the Westwater Canyon Member (sandstone), and the Recapture member (interbedded claystone and sandstone).

The Jackpile Member of the Morrison Formation is the source rock for the uranium production at the Site, with Pit 1 penetrating approximately 75 ft into this unit. The thickness of the exposed Jackpile sandstone in Pit 1 varies from approximately 30 to 80 ft and is representative of deposition in a braided stream environment.

### 2.3 Site Seismicity

A design seismic return period is not specified by local regulations. A 10,000-year return period was chosen based on standard practice for passive closure for mining tailings facilities (GISTM, 2020). The USGS Unified Hazard Tool (<https://earthquake.usgs.gov/hazards/interactive/>) was used to evaluate the seismic hazard for a return period of 10,000 years using the 2014 Revision of Time-Independent Probabilistic Seismic Hazard Maps for the United States. The peak ground acceleration (PGA) for an AEP of  $1 \times 10^{-4}$  is approximately 0.27 g, assuming a generic site condition of 760 m/s. The hazard curves from the USGS Unified Hazard Tool are provided in Figure 3.



**St. Anthony Mine: Pit 1 Highwall Stability – Phase 2 Report**  
**2.0 Site Description**

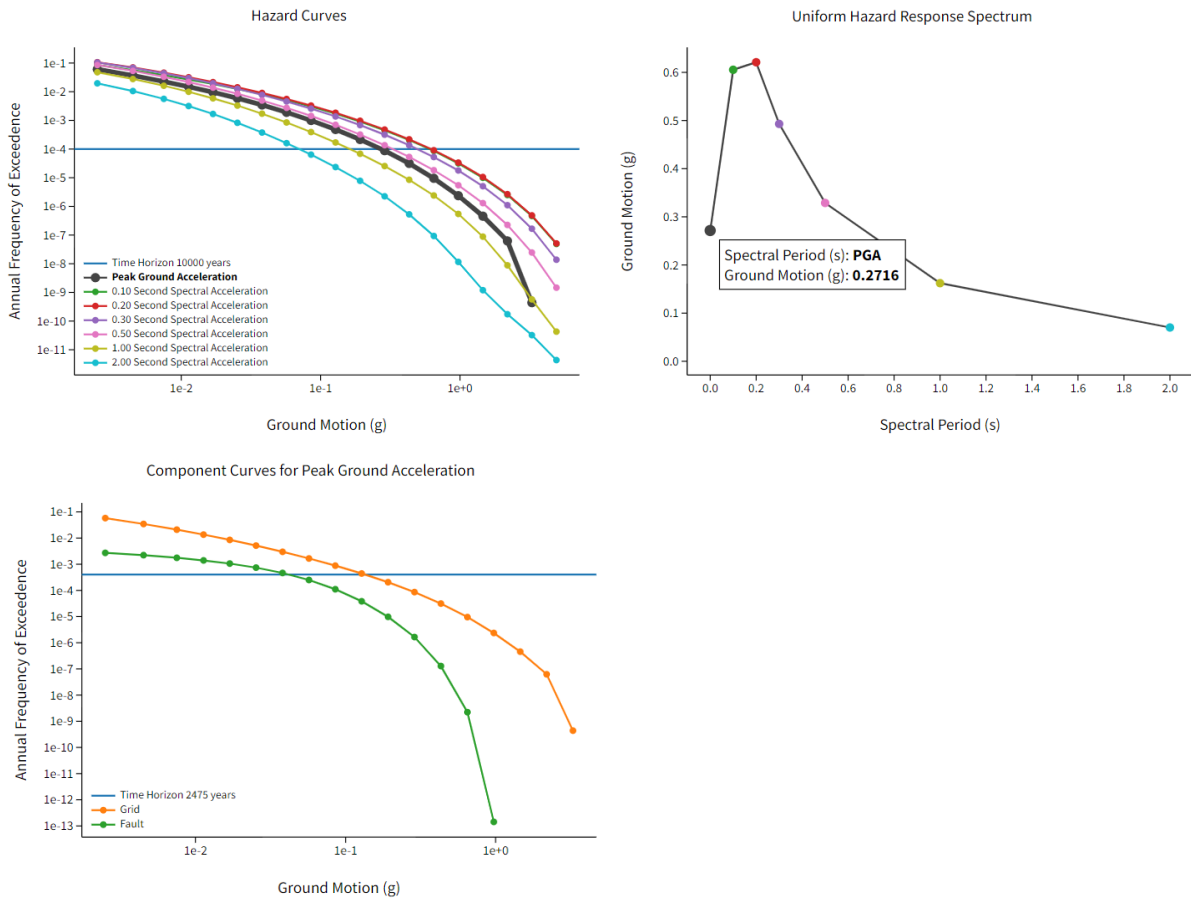


**Figure 3: Hazard Curves from USGS Unified Hazard Tool for the PGA**



### 3.0 GEOTECHNICAL FIELD INVESTIGATION

The geotechnical field investigation took place over the period of 10 November 2021, to 28 January 2022, and consisted of five boreholes. Final borehole depths, inclination, and azimuths are included in Table 1. Dilatometer testing was completed in borehole BH-3 and acoustic and optical televiewer surveys were completed in the two inclined boreholes. The dilatometer testing and televiewer surveys were completed by COLOG.

Final borehole locations were chosen by Stantec and adjusted in the field with input from Authentic drilling regarding access. Borehole locations were surveyed in the field with a handheld GPS unit and are shown on Figure 4 and in Appendix B.

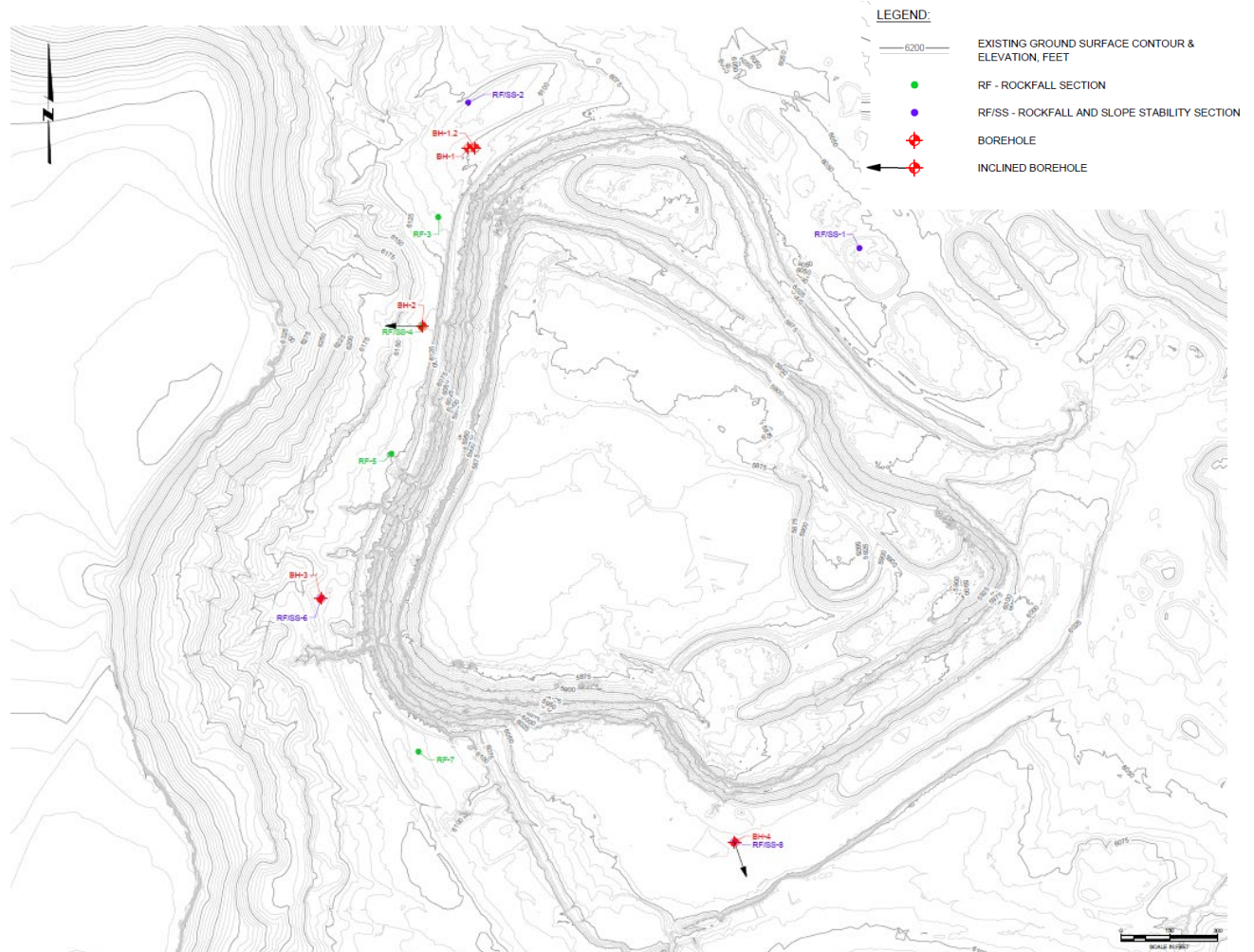


Figure 4: Borehole Location Diagram



### **3.1 Geotechnical Borehole Drilling**

Five boreholes were drilled under the supervision of Stantec personnel. Subsurface conditions were logged in the field by Stantec geologists and/or geotechnical engineers.

The boreholes were advanced with the use of an Acker Renegade track mounted drill rig equipped for geotechnical sampling and testing. Standard penetration tests (SPT) were conducted at 5-foot intervals within the overburden soils, using a 2.5-inch outside diameter (od) split spoon (SS) sampler driven into the soil with blows of a 140-pound hammer falling 30 inches. Bedrock was cored with oversize NQ and HQ diamond drill bits using a triple inner tube system to recover the rock core samples. Drill water was pumped from water totes transported to site each day. After each 5-foot (approximate) drill run was complete, the drill rig operator stopped the rotation of the drill head, disconnected the drill head from the rock coring string, lowered an overshot downhole grapple into the rock coring string on the wireline cable, and winched the inner tube to the surface.

The Total Core Recovery (TCR), Solid Core Recovery (SCR) and Rock Quality Designation (RQD), were measured and recorded by Stantec. Detailed logging for each rock core run was completed in the inner sleeve of the triple tube sampler. Core samples were scanned for radiation using an HP-210L Geiger-Mueller detector provided by AVM Environmental Services. Overburden samples were bagged, and rock core was placed in core boxes and transported to Colorado to finalize logging and select samples for laboratory testing. Overburden samples were selected for classification and index property testing and core samples were selected for strength and durability testing at the laboratory. Core samples selected for strength testing were packaged carefully to minimize breakage. Nine overburden samples and 110 rock core samples were transported to Advanced Terra Testing (ATT) for laboratory testing. A summary of the borehole details is presented in Table 1, and the detailed borehole record is provided in Appendix C. Core photographs are presented in Appendix D. Monster plots and histograms used to visualize borehole data are included in Appendix E.



**St. Anthony Mine: Pit 1 Highwall Stability – Phase 2 Report**  
**3.0 Geotechnical Field Investigation**

**Table 1: Borehole Details**

Area	Borehole Number	Collar Elevation (ft)	Angle (Degrees)	Azimuth (Degrees)	Length (ft)	Sample Types	In-situ Testing
North Highwall	BH-1	6100	0	-	113.5	SS & NQ	-
	BH-1.2	6098	0	-	252.5	NQ	-
West Highwall	BH-2	6130.5	26.1	270.7	302	NQ & HQ	Televiewer
	BH-3	6136	0	-	290	NQ	Dilatometer
South Highwall	BH-4	6041	25.6	160.9	215	HQ	Televiewer

Notes:

Sampling locations are shown on Figure 4

Lengths are total feet of core.

Angle of borehole is measured from vertical (i.e., an angle of 0 degrees represents a vertical borehole)

Azimuth of borehole is measured from north

### 3.2 Acoustic and Optical Televiewer Surveys

Stantec retained COLOG to undertake and interpret acoustic and optical televiewer surveys in boreholes BH-2 and BH-4. The televiewer surveys were carried out on 22 and 28 January 2022 and were completed over the uncased portions of the boreholes. Prior to the surveys, the boreholes were flushed with a flocculent mixed into fresh water to remove as many suspended particles as possible. During the survey, downhole information was collected, including borehole azimuth, tilt, and magnetic field, which was used to orient the structural features picked in the imagery to determine the in-situ dip / dip direction of each structure. By reviewing conditions in the walls of the boreholes, the televiewer surveys capture data in areas of weak rock with low core RQD, which is likely disturbed during diamond drilling. Downhole televiewer logs are presented in Appendix F.

Stantec used the oriented structural data captured by televiewer surveys to undertake kinematic analyses to assess the potential of structurally controlled slope failures and as input into limit equilibrium geotechnical models used to evaluate rock mass slope stability.

### 3.3 Dilatometer Testing

Stantec retained COLOG to undertake dilatometer (DMP) testing in borehole BH-3. The purpose of the DMP testing was to evaluate the elastic moduli of the weak rock materials in-situ, as the weakness of the rock was anticipated to create difficulties finding and transporting intact rock core samples large enough for UCS testing. The elastic modulus of the rock mass is a parameter used in the evaluation of the stability of rock slopes, that can also be measured through elastic laboratory strength testing. Ten DMP tests were performed on 22 November 2021, at depths ranging from 49.6 ft to 139.6 ft using a RocTest Probox dilatometer. The testing methodology and results are presented in Appendix G.



### **3.4 Core Sample Activity Screening**

Stantec scanned core samples for activity levels with an HP-210L Geiger-Mueller detector provided by AVM Environmental Services. Samples from boreholes BH-2, BH-3, and BH-4 were also scanned using a Ludlum 12S microR meter to detect gamma radiation exposure rates in units of micro Roentgen per hour. Gamma screening data is presented in Appendix H and on the borehole logs included in Appendix C.

AVM provided interpretation of the readings taken using the HP-210L detector in comparison to the background readings and classified samples as “near background”, “slightly above background”, or “above background”. These interpretations are presented for each core run in Appendix H and were compared to the current pit bottom elevation at each borehole location as described in Section 5.4.



## 4.0 GEOTECHNICAL LABORATORY TESTING

Laboratory testing for the field program was completed by Advanced Terra Testing in Lakewood, Colorado. Samples were transported to Fort Collins, Colorado after completion of the field drilling program where they were selected and packed before being transported to the lab. Samples were selected to represent each bedrock material type. A majority of samples were selected in the Mancos bedrock unit, since this upper unit is the governing unit for rock mass highwall stability due to its higher elevation along the pit walls and lower strength. Due to the requirement for full diameter core with lengths at least twice the diameter, many samples in the upper 30 ft of the boreholes, particularly in the shale were not testable due to fracturing.

### 4.1 Soil Sample Index Testing

Nine overburden samples were collected using split spoon samplers and bagged in the field before being sent to the lab. Index tests were performed on the overburden samples to classify soils and characterize field conditions. Laboratory tests conducted on the samples included moisture content (ASTM D2216), particle-size distribution with hydrometer (ASTM D7928), and Atterberg Limits (ASTM D4318). Overburden soils generally consisted of silt underlain by sandy or silty clay above the bedrock interface. Laboratory test results are summarized in Table 2.

**Table 2: Soil Sample Index Test Results**

Borehole ID	Depth (ft)	Soil Type	Moisture Content	Liquid Limit	Plasticity Index	% Fines
BH-1	5	Clayey Sand (SC)	5.7	24	7	47.6
BH-1	10	Sandy Lean Clay (CL)	10.3	-	-	-
BH-1	15	Sandy Lean Clay (CL)	12.3	33	16	59.0
BH-1	20	Clayey Sand (SC)	16.2	-	-	-
BH-1	25	Clayey Sand (SC)	10.8	24	7	47.1
BH-3	5	Silty Sand (SM)	3.9	-	-	-
BH-3	10	Silty Sand (SM)	3.0	NL	NP	34.6
BH-3	20	Silty Sand (SM)	7.4	-	-	-
BH-3	25	Sandy Lean Clay (CL)	11.5	26	7	65.5

### 4.2 Point Load Index Testing of Rock Core Samples

Point load tests (PLT) are undertaken to evaluate the strength of the intact rock, in addition and for correlation with laboratory test of rock core samples for unconfined compressive strength. PLT were completed by ATT in accordance with ASTM D5731. Consistent with the ASTM procedure, core specimens with a length / diameter ratio of greater than 2.0 were selected for PLT and were undertaken both diametrically and axially.



**St. Anthony Mine: Pit 1 Highwall Stability – Phase 2 Report**  
**4.0 Geotechnical Laboratory Testing**

During a PLT, a compressive load is applied to the sample through two 60-degree conical shaped platens, which cause the rock to break in tension between these two points. Bedding is near horizontal for vertical boreholes, therefore, an axial point load test ( $Is_{(50)A}$ ) was completed to measure rock index strength perpendicular / normal to the plane of bedding and diametrical point load tests ( $Is_{(50)D}$ ) were completed to measure rock index strength parallel to the plane of bedding.

Test results are reported as a Point Load Index ( $Is_{(50)}$ ) corrected to a standard 50 mm diameter specimen. The size corrected Point Load strength index of a rock specimen is defined as the value that would have been measured in a diametral test with a diameter equal to 50 mm. For the tests on NQ3 and HQ3-sized core specimens, with approximate diameters of 41 mm and 61 mm, respectively, a correction factor was applied, given by the following equation.

$$F = \left(\frac{D_e}{50}\right)^{0.45}$$

With:

F        Size Correction Factor  
D<sub>e</sub>      Equivalent Core Diameter

The equivalent core diameter was 78 to 144 mm for the diametral tests. The axial diameter was determined individually for each sample in accordance with ASTM D5731. PLT results are presented in Appendix I and summarized in Section 5.2.3.

PLT results paired with unconfined compressive strength (UCS) tests completed on nearby samples were used to establish a correlation and calculate compressive strength from  $Is$  values. As described in Section 5.2.3, the calculated compressive strengths were used along with UCS results to define material compressive strengths for slope stability analyses.

### **4.3 Unconfined Compressive Strength of Rock Core Samples**

Twenty-four rock core samples were selected for measurement of the UCS of the intact rock with strain measurements (ASTM D7012 Method D) at ATT.

Strain gauges were mounted on each prepared core sample. Axial load was applied continuously at a rate of approximately 1,000 to 3,000 lb/min, and the maximum load sustained prior to failure by the specimen was recorded. Elastic moduli were then calculated for each specimen. The test results are presented in Appendix I and summarized in Section 5.2.3.

Nineteen rock core samples were prepared and tested for UCS in accordance with ASTM D7012, Method C at ATT. Method C does not include the use of strain gauges; therefore, a stress-strain curve is not produced. The test results are presented in Appendix I and summarized in Section 5.2.3.



UCS and elastic modulus of the intact rock determined from the laboratory test results were used along with PLT to develop input values for the slope stability assessment as described in Section 5.2.3.

#### **4.4 Triaxial Compressive Strength of Rock Core Samples**

Triaxial tests are performed to evaluate the compressive strength and elastic moduli of rock samples. Three rock core samples were selected for triaxial compressive strength testing (ASTM D7012, Method B). The rock core samples were confined to pressures of 350, 750, and 1,500 psi and axial load was applied at a rate of 9,000 to 12,000 lb/min. Both axial and lateral strain data were used to create a stress strain curve which was used to determine the elastic modulus of each rock sample. Results of the triaxial testing are shown in Table 3.

**Table 3: Triaxial Compressive Strength Test Results**

<b>Borehole ID</b>	<b>Depth (ft)</b>	<b>Rock Type</b>	<b>Density (lb/ft<sup>3</sup>)</b>	<b>Confining Pressure (psi)</b>	<b>Effective Stress (psi)</b>	<b>Poisson's Ratio</b>	<b>Young's Modulus (psi)</b>
BH-1.2	117	Mancos Shale	148.7	350	7900	0.053	960000
BH-3	126	Mancos Siltstone	147.7	750	9517	0.158	1190000
BH-3	178	Mancos Sandstone	126.4	1500	10534	0.129	2070000

#### **4.5 Direct Shear Strength of Rock Core Samples**

Direct shear tests (ASTM D5607) were undertaken on eleven rock discontinuity samples to evaluate shear strength along joints. All direct shear samples were identified as open joints during core logging. Each sample was sheared under three different normal stresses. Normal stresses ranged from 21 psi to 330 psi based on approximate in-situ field stresses. Stantec applied correction factors for vertical dilation, using the Hencher method (Hencher, 1995). Peak and residual shear stress values were identified for each normal stress to evaluate the peak and residual friction angle. Direct shear results for the Mancos formation were used to define the bedding strength for anisotropic rock conditions.

#### **4.6 Durability Testing of Rock Core Samples**

Three rock core samples were selected for wet-dry durability testing (ASTM D5313), two samples were selected for freeze-thaw durability testing (ASTM D5312), and five samples were selected for slake durability testing (ASTM D4644). Durability samples were chosen from near surface Mancos formation units. The wet-dry and freeze-thaw samples disintegrated within the first cycle. The slake durability test results are presented in Appendix I. These test results are used to evaluate the rock for erosion and weathering susceptibility; they were not used in the stability models but indicate the selected samples are susceptible to erosion and weathering over time.



## **5.0 SUMMARY OF SUBSURFACE CONDITIONS**

### **5.1 Overburden**

Approximately 1 to 30.5 ft of overburden soils were encountered at the surface of two of the four boreholes. Overburden samples were collected in boreholes BH-1 and BH-3 and were classified using the index testing. The overburden soils generally consisted of medium dense to dense silty sand or clayey sand with occasional zones of very stiff sandy lean clay.

### **5.2 Bedrock**

The bedrock consisted of shale, siltstone, and sandstone within the Mancos formation, underlain by primarily sandstone within the Dakota and Jackpile formations. The Brushy Basin formation was encountered below the Jackpile in three of the boreholes. The Mancos shale was clayey and highly weathered near the surface to depths of approximately 28 to 42 ft. The Mancos formation was thinly bedded, and the siltstone and sandstone units were fine grained. The Mancos siltstone and sandstone units were similar in structural and strength characteristics and were grouped together for defining model parameters as described in the following sections. The Dakota sandstone was fine grained with thin shale interbeds. The Jackpile sandstone was fine to medium grained and poorly cemented / friable.

The major joint set is along near horizontal bedding planes with occasional near vertical joints towards the top of the highwall. Partially to fully healed vertical joints with gypsum infill were encountered within the Mancos formation.

The bedrock is relatively flat however the top surface of the Mancos bedrock generally slopes to the southeast and the Dakota and Jackpile formations generally dip to the northeast in the vicinity of Pit 1. A summary of the observed bedrock stratigraphy is presented in Table 4. Borehole logs and photos of the rock core samples are provided in Appendix C and Appendix D, respectively.



**St. Anthony Mine: Pit 1 Highwall Stability – Phase 2 Report**  
**5.0 Summary of Subsurface Conditions**

**Table 4: Bedrock Stratigraphy**

Rock Formation	Top Elevation (ft)	Bottom Elevation (ft)	Thickness (ft)
Overburden	6040-6136	6030-6129	1-31
Mancos Sandstone (BH-2 upper layer)	6129	6108	21
Mancos Shale	6070-6108 (upper) 5989-6001 (lower)	6030-6043 (upper) 5972-6004 (lower)	39-77 (upper) 11-27 (lower)
Mancos Sandstone & Siltstone	6030-6043 (upper) 5972-6004 (lower)	5989-6001(upper) 5926-5955 (lower)	30-45 (upper) 45-49 (lower)
Dakota Sandstone	5926-5955	5907-5941	14-18
Jackpile Sandstone	5907-5941	5847-5852	54-88
Brushy Basin	5847-5852	-	-

**5.2.1 Total Core Recovery, Solid Core Recovery and Rock Quality Designation**

Total Core Recovery (TCR), Solid Core Recovery (SCR), and Rock Quality Designation (RQD) were measured for the completed boreholes and are shown on the borehole logs in Appendix C. Detailed logging of joints and RQD measurements were based on field judgement on whether joints observed in core samples were in-situ or mechanically induced by drilling activities. This judgement was challenging due to near horizontal rock bedding and overall weak rock strength. Detailed joint logging data and RQD/SCR measurements from the core should be considered approximate. Televiewer data from BH-2 and BH-4 were reviewed and used to adjust RQDs for mechanical failures. The average TCR, SCR, and RQD for each formation are summarized in Table 5.



**St. Anthony Mine: Pit 1 Highwall Stability – Phase 2 Report**  
**5.0 Summary of Subsurface Conditions**

**Table 5: TCR and RQD**

Borehole ID	Formation Description	Depth (ft)	TCR <sup>1</sup> (%)	SCR <sup>2</sup> (%)	RQD <sup>3</sup> (%)
BH-1	Mancos Weathered Clayey Shale	36.5-52.5	79.0	75.0	71.0
	Mancos Shale	52.5-69.5	97.2	97.2	89.6
	Mancos Siltstone & Sandstone	69.5-112.1	98.0	98.0	96.6
BH-1.2	Mancos Shale	109-123.3	68.1	52.7	5.7
	Mancos Siltstone & Sandstone	123.3-172.3	99.1	98.9	71.0
	Dakota Sandstone	172.3-190.6	97.9	97.9	97.7
	Jackpile Sandstone	190.6-246.3	64.8	64.8	64.8
	Brushy Basin	246.3-252.5	93.3	93.3	93.0
BH-2	Mancos Sandstone	15-24.8	84.0	71.8	78.3
	Mancos Shale	24.8-110.8	45.4	43.3	43.0
	Mancos Siltstone & Sandstone	110.8-143.6	99.0	96.1	98.2
	Mancos Shale	143.6-175.6	97.9	97.7	97.0
	Mancos Siltstone & Sandstone	175.6-225.5	100.0	100.0	100.0
	Dakota Sandstone	225.5-241.5	100.0	100.0	93.6
	Jackpile Sandstone	241.5-302	61.9	61.9	61.9
BH-3	Mancos Weathered Clayey Shale	36.1-42.0	98.2	85.9	83.7
	Mancos Shale	42.0-87.1	94.2	86.3	89.1
	Mancos Siltstone & Sandstone	87.1-136.7	99.0	98.3	98.8
	Mancos Shale	136.7-147.4	100.0	100.0	97.4
	Mancos Siltstone & Sandstone	147.4-192.1	99.3	99.1	99.4
	Dakota Sandstone	192.1-207.0	90.7	87.4	90.7
	Jackpile Sandstone	207.0-289.2	81.4	78.2	81.4
BH-4	Mancos Weathered Clayey Shale	16.0-28.5	44.6	41.8	43.3
	Mancos Shale	28.5-41.0	100.0	90.7	100.0
	Mancos Sandstone	41.0-95.4	99.0	99.0	98.5
	Dakota Sandstone	95.4-111.0	96.4	96.4	84.1
	Jackpile Sandstone	111.0-209.5	94.3	94.2	90.6
	Brushy Basin	209.5-215.0	100.0	100.0	75.0

Notes:

Weighted average of Total Core Recovery (TCR)

Weighted average of Solid Core Recovery (SCR)

Weighted average of Rock Quality Designation (RQD)



### 5.2.2 Geological Strength Index

The Geological Strength Index (GSI) is a rock mass classification system that is based on a qualitative description of a rock mass, as described in Marinos et al., 2007. GSI is used as an input to the Hoek Brown rock mass empirical strength estimation. Estimation of GSI was carried out using two methods listed below.

- Visual assessment of the rock mass, using photographic observations along the exposed rock faces in Pit 1 and on rock core data and photographs, using the GSI chart developed by Marinos and Hoek (Hoek, 2019). Core photographs are included in Appendix D and the GSI charts are provided in Appendix J.
- Quantification using empirical relationships, developed by Hoek et al. (2013) between the GSI and rock properties determined from rock core, including the RQD index and the joint condition rating (JCon<sub>89</sub>). The relationship is described with the following formula.

$$GSI = 1.5JCon_{89} + RQD/2$$

Where:

GSI = Geological Strength Index.

JCon<sub>89</sub> = Joint Condition Rating based on the Rock Mass Rating (RMR<sub>89</sub>) system (Bieniawski, 1989).

RQD = Rock Quality Designation Index, determined from rock core during 2021 investigation.

The Joint Condition Rating used to calculate GSI was developed using the qualitative rock core data collected during the drilling investigation.

GSI values were estimated for each geological formation encountered in the 2021-22 drillholes for use in the stability analysis and are provided in Table 6. Further details on the inputs used for the assessment are provided in Appendix J.

**Table 6: Geological Strength Index (GSI) values**

Formation/Lithology	GSI Used in Analysis (Marinos and Hoek, 2000 chart)		GSI (based on Hoek et al. 2013)	
	Lower Bound	Average	Lower Bound	Average
Mancos Shale	30	35	59	63
Mancos Siltstone & Sandstone	35	45	76	84
Dakota Sandstone	40	45	72	85
Jackpile Sandstone & Brushy Basin	50	55	70	80

GSI values determined using the 2013 correlation were nearly two times higher than GSI values determined using existing pit wall observations and core photographs. This variability is likely due to the limited rock core data compared to visual highwall data. RQD and JCon<sub>89</sub> values used to calculate the 2013 GSI were estimated based on field judgements during detailed core logging,



## St. Anthony Mine: Pit 1 Highwall Stability – Phase 2 Report

### 5.0 Summary of Subsurface Conditions

with some degree of uncertainty and the scale of the wall rock compared with the core. Additionally, it should be noted that the 2013 correlation was developed for underground tunnels. GSI values are highly dependent on the scale or joint spacing relative to the slope or tunnel surface being evaluated. The empirical relationship developed for tunnels may overestimate GSI for a larger scale highwall. Since the GSI values determined from the chart are lower values, these were adopted in the stability analysis.

#### 5.2.3 Unconfined Compressive Strength

Unconfined compressive strength (UCS) values for intact rock core specimens were obtained from laboratory UCS and point load tests (PLT). The combined UCS and PLT tests with UCS correlations were analyzed for each geological formation. Point load test results were analyzed based on the procedures outlined in ASTM D5731, considering the following.

- PLT are only applicable to rocks of medium compressive strength or greater ( $> 15$  MPa). PLT results below 15 MPa were not included in the compressive strength data analysis per ASTM D5731. A majority of the PLT results below medium strength were Mancos Shale samples.
- Notable point load value outliers were disregarded for the determination of the average PLT conversion factor.
- Correlations between UCS lab tests and PLT field tests were based partner samples that were taken from the same location (within 3 ft of the rock core). Correlation factors K ranging from 28-30 were determined and then used for each formation to extrapolate point load index to UCS.
- The UCS of intact rock by formation, based on laboratory UCS tests and correlated field point load tests, is summarized in Table 7. The Mancos sandstone and siltstone formations were grouped together for stability analysis due to comparable UCS results and structural characteristics.

The removal of invalid PLT results below 15 MPa from the data analysis appears to have biased correlation factors and overall strength results towards higher compressive strengths. As shown in Table 7, the strengths from PLT tests for Mancos Shale and Jackpile Sandstone are almost twice the strengths from UCS tests. For these two materials, the average compressive strengths from only the UCS tests were used as conservative values in the model. For the remaining materials, the average of all UCS and PLT results were used in the model. Lower bound UCS results were used for weak layers in the model as described in Section 7.5.2.

Additionally, portions of the Mancos shale within the upper 20 to 30 ft of each borehole were not testable for PLT or UCS due to poor quality samples. Borehole logs indicated weak to very weak shale in these portions of the logs. An average strength was applied to the Mancos shale in the model based on samples collected at depths ranging from approximately 25 to 145 ft and weaker portions of shale in the upper 20 to 30 ft of the highwalls may have lower strengths. This small



**St. Anthony Mine: Pit 1 Highwall Stability – Phase 2 Report**  
**5.0 Summary of Subsurface Conditions**

portion of the highwall would generally be less than one full bench and is unlikely to have a significant impact on global stability.

**Table 7: Unconfined Compressive Strength (UCS) Test Results**

Formation	Unconfined Compressive Strength (laboratory UCS tests)			Unconfined Compressive Strength (point load tests) <sup>1</sup>		
	No. of tests	Range (ksf)	Average (ksf)	No. of tests	Range (ksf)	Average (ksf)
Mancos Shale	5	443-835	636	4	539-1775	1027
Mancos Siltstone	9	729-992	865	4	555-823	751
Mancos Sandstone	16	105-1261	771	12	414-1665	965
Dakota Sandstone	2	1287-1917	1602	1	508	-
Jackpile Sandstone	7	282-649	490	3	590-1320	837

<sup>1</sup> A site specific correlation factor of K = 30 was used to estimate UCS values from the uncorrected point load strength index values I<sub>s</sub> for Mancos Shale, Siltstone, and Sandstone. K=28 was used to calculate UCS values from I<sub>s</sub> for Dakota Sandstone and Jackpile Sandstone. The site-specific correlations factors were calculated from paired PLT and UCS tests in accordance with ASTM D5731.

**5.2.4 Discontinuities**

The orientations (dip and dip direction) of the discontinuities encountered in the boreholes were identified from the televiewer data collected in boreholes BH-2 and BH-4 and from the ShapeMetrix<sup>3D</sup> model, which collected data from a drone survey of the highwalls. ShapeMetrix<sup>3D</sup> data collection was limited to areas of exposed outcrop. Surfaces in the exposed sandstone were primarily used to measure structural orientations due to their relative resistance to erosional forces compared to shale. In total, the orientation (dip and dip direction) of 179 discontinuities were measured from the ShapeMetrix<sup>3D</sup> models and field mapping, an example of the structural measurement is shown in red in Figure 5. Televiewer data identified 539 discontinuities in BH-2 and 330 discontinuities in BH-4. Only 89 of the discontinuities in BH-2 and 20 of the discontinuities in BH-4 were identified by Colog as partial to fully open fractures, the remainder were identified as healed fractures or bedding planes.

The oriented data was plotted on a stereonet for visualization and interpretation. A Terzaghi weighting was applied to the borehole televiewer data to account for any sampling bias due to data collection along vertical boreholes. The stereoplots of the weighted oriented discontinuity televiewer and ShapeMetrix<sup>3D</sup> data are provided in Figure 6 and Figure 7. The discontinuities in the rock mass are dominated by the sub-horizontal bedding of the sedimentary formations. Approximately 732 of the total 1,048 discontinuities were identified as a set of sub-horizontal bedding discontinuities. A separate stereonet with bedding discontinuities filtered out was developed to identify smaller subsets of discontinuities. Tables 8 and 9 summarize the characteristics of the dominant joint sets observed.



**St. Anthony Mine: Pit 1 Highwall Stability – Phase 2 Report**  
**5.0 Summary of Subsurface Conditions**

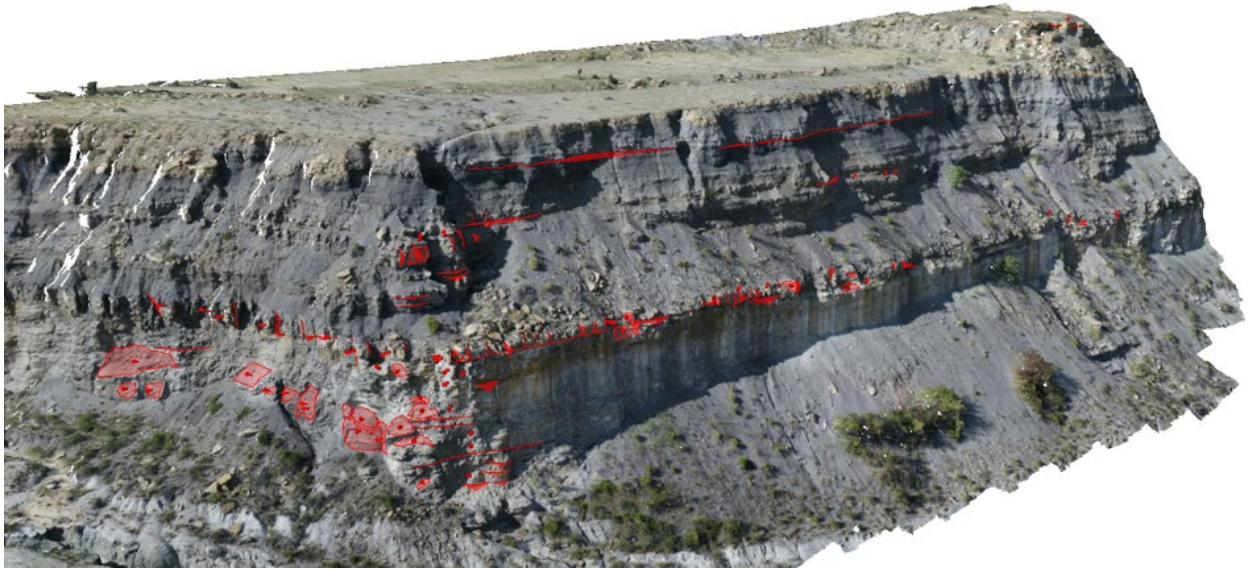


**Figure 5: ShapeMetrix3D Model**



**St. Anthony Mine: Pit 1 Highwall Stability – Phase 2 Report**  
**5.0 Summary of Subsurface Conditions**

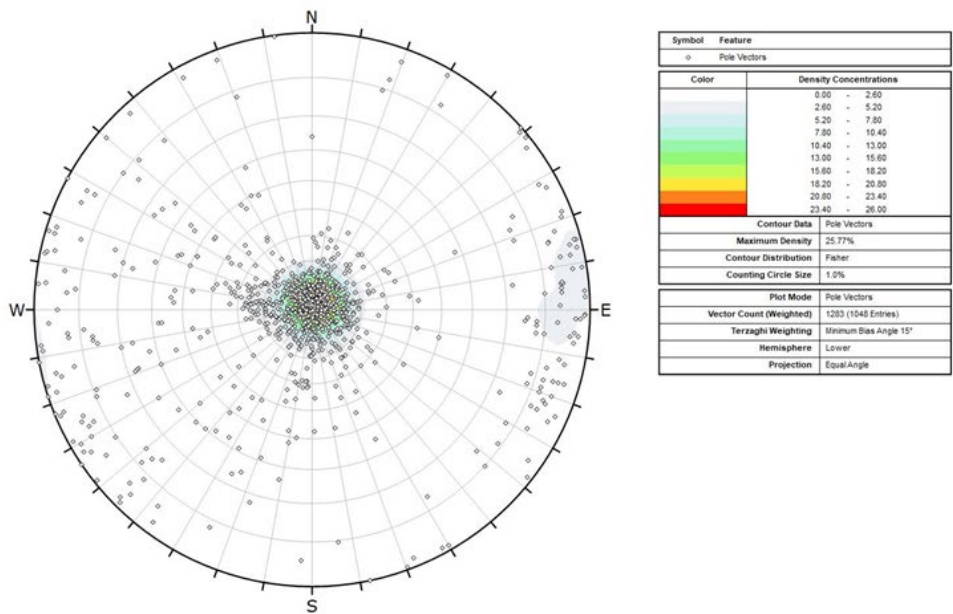


**Figure 6: Stereographic Plot with All Discontinuities**

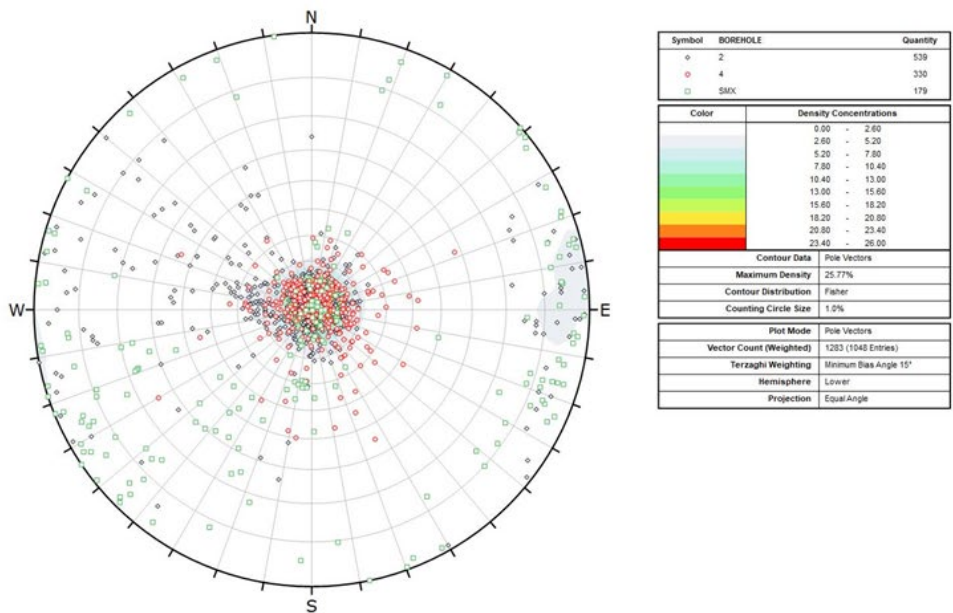


**Figure 7: Symbolic Stereographic Plot with All Discontinuities**



**St. Anthony Mine: Pit 1 Highwall Stability – Phase 2 Report**  
**5.0 Summary of Subsurface Conditions**

The discontinuities in the rock mass are dominated by the sub-horizontal bedding of the sedimentary rock formations, as illustrated in Figure 6 and Figure 7. The dominant set of discontinuities, identified in Figure 8 as  $S_0$ , is sub-horizontal bedding planes with a dip of 2 degrees  $\pm$  10 degrees and dipping toward the southwest. Smaller subsets of discontinuities, identified in Figure 9 below as  $J_1$ ,  $J_2$  and  $J_3$  have a mean dips ranging from 36 to 88 degrees  $\pm$  20 degrees. Set  $J_1$  dips steeply toward to the west and partly overturned toward the east. Sets  $J_2$  and  $J_3$  dip to the east and north, respectively. The remaining discontinuities dip at various angles in different directions without appearing to form distinct discontinuity sets. Discontinuities both within sets and outside of sets were evaluated in the kinematic analysis described in Sections 6.1 and 6.2.

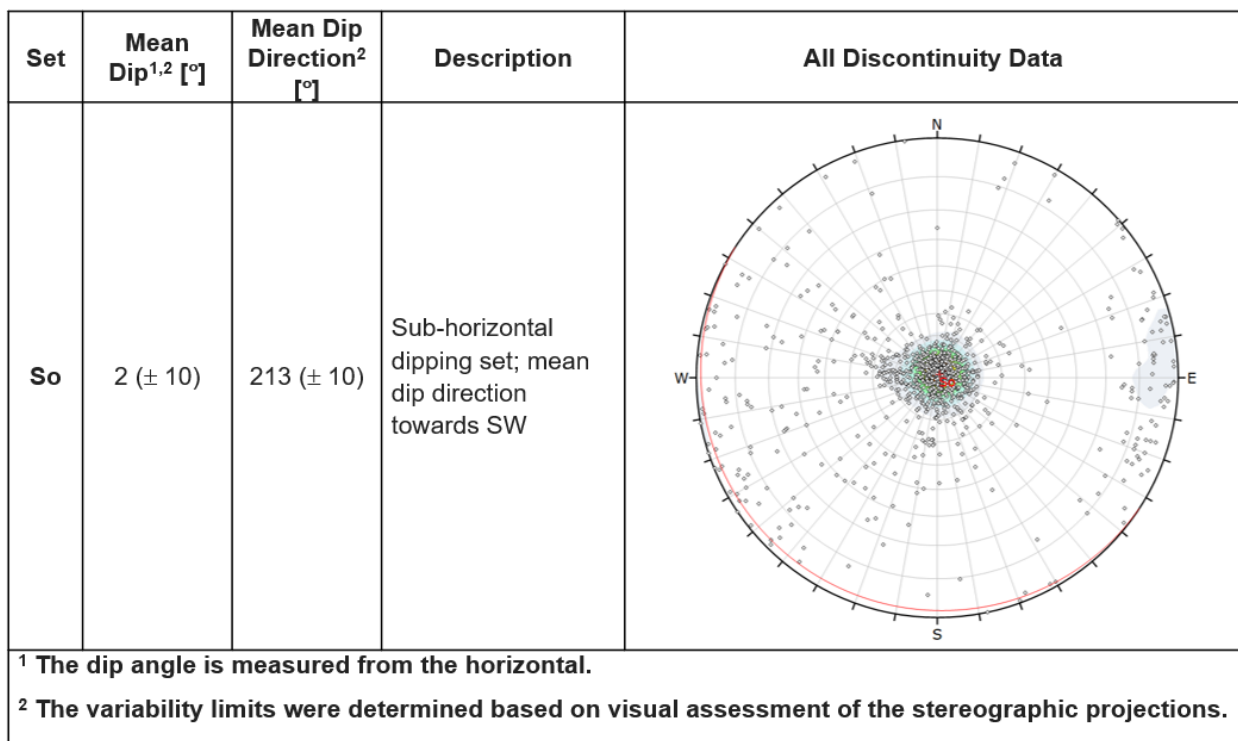


**Figure 8: Bedding Discontinuity Orientation Summary**



**St. Anthony Mine: Pit 1 Highwall Stability – Phase 2 Report**  
**5.0 Summary of Subsurface Conditions**

Set	Mean Dip <sup>1,2</sup> [°]	Mean Dip Direction <sup>2</sup> [°]	Description	Discontinuity Data Excluding Bedding
J1	88 (± 20)	267 (± 30)	Steeply dipping set; mean dip direction towards W, partly overturned dipping toward E	
J2	36 (± 20)	108 (± 30)	Moderately dipping set; mean dip direction towards E	
J3	41 (± 20)	18 (± 30)	Moderately dipping set; mean dip direction towards N	

<sup>1</sup> The dip angle is measured from the horizontal.  
<sup>2</sup> The variability limits were determined based on visual assessment of the stereographic projections.

**Figure 9: Joint Sets Discontinuity Orientation Summary**

**5.2.5 Discontinuity Strength**

Discontinuity parameters including shape, roughness, character, surface condition, infilling type and filling width were recorded during detailed core logging. Guidelines from the International Society for Rock Mechanics (ISRM, 2007) were used to provide qualitative discontinuity descriptions.

A majority of discontinuities were either planar or undulating in shape, with smooth or rough surfaces. Near surface discontinuities within the Mancos formation were typically infilled with gypsum. A majority of discontinuities were clean or slightly stained. Barton-Bandis shear strength parameters were determined using the Joint Roughness Coefficient (JRC) and Joint Wall Condition Strength (JCS) observed during core logging and verified through laboratory direct shear testing.

The shear strength of discontinuities is a function of the in-situ conditions such as roughness, wall strength and the applied normal stresses. The strength characteristics of discontinuities can be described using the empirical Barton-Bandis failure criterion in which the shear strength ( $\tau$ ) along the sliding surface is expressed in terms of the Joint Roughness Coefficient (JRC), the Joint Wall Compressive Strength (JCS) and the residual friction angle of the failure surface ( $\phi_r$ ).



**St. Anthony Mine: Pit 1 Highwall Stability – Phase 2 Report**  
**5.0 Summary of Subsurface Conditions**

The shear strength developed when an effective normal stress ( $\sigma_n$ ) is acting on a sliding surface is expressed as the following (Barton and Choubey, 1977).

$$\tau = \sigma_n \tan \left[ \phi_r + JRC \log_{10} \left( \frac{JCS}{\sigma_n} \right) \right]$$

Laboratory direct shear strength results for Mancos Shale and Sandstone samples were used to determine the shear strength along joints. Average and lower bound residual friction angles  $\phi_r$  of 24.6° and 15.9°, respectively, were determined from the direct shear test results for Mancos Shale. Average and lower bound residual friction angles  $\phi_r$  of 28.5 and 19.4, respectively were determined for the Mancos Sandstone.

Mancos shale Barton-Bandis anisotropic parameters provided in Table 8 were input into RSDData™ software from Rocscience. Normal versus shear stress functions output from the RSDData Barton-Bandis model were used to assign bedding strength properties to the Mancos Shale in the slope stability analyses using a Snowden anisotropic strength model.

**Table 8: Discontinuity Input Parameters**

Criteria		Parameters	Average <sup>2</sup>	Lower Bound <sup>3</sup>
Input Parameters	Barton-Bandis Criterion	Residual Friction angle (degrees) <sup>1</sup>	24.6	15.9
		Joint Roughness Condition (JRC)	16	9
		Joint Wall Compressive Strength (JCS) (ksf)	636	429

<sup>1</sup> The residual friction angle was estimated from the average and lower bound direct shear test results.

<sup>2</sup> Average values were used to model Mancos Shale bedding strength.

<sup>3</sup> Lower bound values were used to model bedding strength for weak layers of Mancos Shale in the model.

### 5.3 Groundwater Condition

Boreholes for this investigation were drilled using the mud rotary method with fluid flush. Therefore, groundwater measurements were not made during drilling. As described in the Stage 2 Abatement Plan, “the Large Pit (Pit 1) acts as a groundwater sink because the rate of evaporation is greater than the rate of groundwater inflow into the Pit” (INTERA, 2015). The hydraulic sink draws water levels to lower elevation near the center of the pit and creating a cone of depression. There are no monitoring wells within the pit. The water table within the pit was assumed to be relatively flat lying along the pit floor and was estimated from aerial photos of the ponded water. Groundwater levels behind the highwall were estimated for the models using groundwater contours developed in the INTERA groundwater models (INTERA, 2015).



## **5.4 Core Sample Activity Measurements**

Core sample screening data was interpreted by AVM and reviewed by Stantec for general trends related to bedrock formations and elevations along the highwall. In general, the Mancos and Dakota units were at, or near, background radiation. A couple of runs at random elevations within the Mancos and Dakota units in BH-1.2 and BH-3 were slightly above background with activity measurements from 90 to 120 counts per minute (CPM). Background measurements during the core sample scanning ranged from 60 to 80 CPM.

The ore-bearing Jackpile formation ranged from near background to above background radiation levels. Levels in the Jackpile formation generally increased with depth. Exposed Jackpile above the pit floor had near, or slightly above, background levels for each of the core holes except for the hole located along the South Highwall. The deepest Jackpile samples in BH-1.2 and BH-2, located approximately 35 and 10 ft below the current bottom of pit, respectively, were above background levels. Eighteen Jackpile samples from BH-4 sample from approximately 66 ft above the current pit floor to approximately 15 ft below the pit floor had above background activity readings ranging from 100 to 2,500 CPM. Background measurements for BH-4 ranged from 50 to 100 CPM. It should be noted that BH-4 was drilled at an approximate 25.6-degree angle, from vertical to the southeast, in the general direction of the underground mine workings and Pit 2.



## 6.0 SLOPE STABILITY ANALYSIS

### 6.1 Kinematic Analysis

A kinematic analysis was undertaken to evaluate the potential for structurally controlled slope failures, using the discontinuity information gathered from the site investigation. Basic mechanisms of structurally controlled failure are described in detail in *Phase 1 Highwall Stability Report, Section 5.2* dated 05 May 2021. Structurally controlled failure is a function of the discontinuities that dissect a rock mass and the orientation of the slope. Kinematic analyses are undertaken using stereographic projections to identify potential failure modes based on the orientations and frequency of joints. This analysis was performed generally following the guidance in *Rock Slope Engineering* (Wyllie, 2018).

The kinematic analysis was carried out using the software Dips 8.0, an industry standard stereographic projection and kinematic analysis tool from Rocscience to evaluate the potential for planar, wedge, and toppling failure modes using stereographic projections. The results of the kinematic analysis are presented in Appendix K and are further discussed in the following sections.

The kinematic analyses included using the following assumptions and guiding principles.

- In practice, it has been observed the planar failure tends to occur only if the dip of a plane is within a certain angular range of the slope face dip direction (Wyllie and Mah, 2018). For the planar failure analysis, a lateral limit of 20° has been used (i.e., the dip direction of the planar discontinuity must be within 20° of the dip direction of the slope face).
- For true planar sliding on a single plane, a release mechanism (e.g., daylight surface, lateral joints, tension cracks or other mechanism) must exist to enable sliding of a block or rock mass on a single plane to occur. The presence of a release mechanism is challenging to identify from limited borehole data. The kinematic analysis conservatively assumes that release planes exist in the model regardless of actual conditions.
- The overall inclination and azimuths of all highwall slopes were estimated from light detection and ranging (LiDAR) and photogrammetry models. The kinematic analysis was divided into three general highwall orientations, as illustrated in Figure 1: North, West, South, and Northeast Highwalls. The inclination of the bench faces was assumed to be 56° from the horizontal and the following azimuths were assumed.
  - West Highwall: 99°
  - South Highwall: 9°
  - North Highwall: 205°
  - Northeast Highwall: 240°



**St. Anthony Mine: Pit 1 Highwall Stability – Phase 2 Report**  
**6.0 Slope Stability Analysis**

The shear strength along the discontinuities was assumed to be represented by a friction angle of 24.6° and a cohesion of 0 kPa based on the direct shear test results for Mancos Shale. It should be noted that the steeper discontinuities generally consisted of Mancos Sandstone which had an average friction angle of 28.5°.

**6.2 Results of Kinematic Analysis**

The results of the kinematic analyses are summarized in Table 9 and Table 10 and the associated stereoplots are presented in Appendix K. Kinematic analyses were completed for all discontinuities using the stereonet that includes bedding discontinuities. Kinematic analyses for discontinuities in joint sets were completed using the stereonet with bedding discontinuities filtered out.

**Table 9: Results of the Kinematic Analysis for All Discontinuities**

Area	Percent of Planes Within Potential Failure Regions			
	Planar Sliding	Direct Toppling	Flexural Toppling	Wedge Sliding
West Highwall	3% of all poles	0.2% of all intersections	8.0% of all poles	3.0% of all intersections
South Highwall	1% of all poles	1.0% of all intersections	0.5% of all poles	3.0% of all intersections
North Highwall	1% of all poles	0.8% of all intersections	1.0% of all poles	2.0% of all intersections
Northeast Highwall	1% of all poles	0.5% of all intersections	4.0% of all poles	1.5% of all intersections

**Table 10: Results of Kinematic Analysis for Discontinuities in Joint Sets**

Area	Percent of Planes Within Potential Failure Regions	
	Planar Sliding	Flexural Toppling
West Highwall	60% of poles in set J <sub>2</sub>	45% of poles in set J <sub>1</sub>
South Highwall	46% of poles in set J <sub>3</sub>	-
North Highwall	-	13% of poles in set J <sub>3</sub>
Northeast Highwall	-	18% of poles in set J <sub>1</sub>

The percentages give an estimate of percent of discontinuity planes within a potential failure region with respect to all the discontinuities mapped for the site but does not represent a probability of failure. The presence of the discontinuities within potential failure regions does not inherently result in failure but indicates potential planes of weakness which may contribute to failures in the rock face. Approximately 220 out of the total 1,048 discontinuities mapped did not belong to joint sets. Percentages of planes in failure regions were determined for all discontinuities and for joints within identified sets. Percentages for all discontinuities and for sets of discontinuities are identified above in Tables 9 and 10, respectively.



## St. Anthony Mine: Pit 1 Highwall Stability – Phase 2 Report

### 6.0 Slope Stability Analysis

The results of the kinematic analysis using the stereographic projections are summarized by the following.

- There is potential for planar failure in set  $J_2$  along the west highwall. The mean orientation of this joint set is susceptible to planar failure. The results of the planar analysis are presented in figure KIN\_W\_PL\_J2.
- There is potential for planar failure in set  $J_3$  along the south highwall. The mean orientation of this joint set is susceptible to planar failure. The results of the planar analysis are presented in figure KIN\_S\_PL\_J3.

There is potential for flexural toppling failures in set  $J_1$  on the west highwall. The mean orientation of this joint set is susceptible to planar failure. The results of the flexural toppling analysis are presented in figure KIN\_W\_FT\_J1.

The sub-horizontal major discontinuity set (bedding) observed in the boreholes and ShapeMetrix 3D data does not support kinematic sliding failures along the discontinuities, such as planar and wedge sliding failures because the near horizontal dip angle is much lower than the estimated residual friction angle.

The moderately dipping joint sets identified as  $J_2$  and  $J_3$  are oriented within potential planar failure planes along the west and south highwalls, respectively. Set  $J_2$  primarily consists of healed joints located in the Dakota and Jackpile formations. For planar failure to occur, the rock mass driving force would have to overcome the frictional resistance of healed joints. Additionally, discontinuities in these formations would need to daylight along the highwall, evidence of continuous joint sets through the overlying Mancos formation was not observed. Set  $J_3$  primarily consists of ShapeMetrix data, televiewer discontinuities in this set are primarily healed joints. In general, the number of discontinuities in this set is relatively small and would not be expected to cause large-scale planar slope failure.

The steeply dipping joint set identified as  $J_1$  contributes to a blocky nature of the rock mass where it intersects the flat lying bedding set. This promotes surficial gravity falls or toppling failures, with sub-horizontal bedding planes acting as base planes. Toppling or gravity failures along exposed rock faces are typically surficial failures, and the steeply dipping joint sets are not expected to cause large-scale slope failures due to their steepness and intermittent nature.

The kinematic analyses did not identify significant percentages of discontinuities within potential failure planes. The most predominant structurally controlled failure modes observed in the pit are planar and toppling type failures for the West Highwall as supported by the kinematic analyses.

### 6.3 Potential Instabilities Involving Major Structures

No major structural features, such as fault zones, were noted during the Phase 2 drilling investigation or Phase 1 field mapping. Therefore, large-scale failures involving major structures appear unlikely based on the structural interpretation.



## St. Anthony Mine: Pit 1 Highwall Stability – Phase 2 Report

### 6.0 Slope Stability Analysis

Surficial structural features were observed in the field and from drone footage during Phase 1. For detailed observations and photos refer to the *St. Anthony Mine Phase 1 Pit 1 Highwall Stability Report* (Stantec, 2021) included in Appendix A. A majority of the surficial features described below were observed within the Mancos formation with occasional surficial undermining and erosional features observed in the Dakota and Jackpile formations. Surficial features in the Dakota and Jackpile formations were primarily observed along the West Highwall. Surficial structural features included steeply inclined joint sets intersecting with the horizontal bedding features to create block structures. Some surficial rock columns were partially separated from the West Highwall along tension cracks. Erosion and raveling were noted along the highwall faces, particularly along the West Highwall. Undercut zones of rock and small ledges were observed along all highwall faces. Evidence of minor surficial bench and crest failures was observed at various highwall locations along with rockfall debris. The surficial observations indicate zones of surficial instability due to erosion and weathering.

#### 6.4 Slope Stability Analysis

Rock mass slope failures are governed by the rock mass strength and the orientation and properties of discontinuities observed in the rock mass. Failure along discontinuities was analyzed using kinematic analysis. As discussed in Section 6.2, the most predominant failure mode is structural toppling along steeply dipping joint sets. Rock mass stability, where failure of the slope is through the rock mass, is assessed using 2D limit equilibrium analyses.

Five cross-sections along the north, west, south, and east highwalls were selected for stability analysis. Slopes were analyzed for both shallow failures along the surface, or failure of a single bench, and global failures deeper into the highwall through multiple benches.



**St. Anthony Mine: Pit 1 Highwall Stability – Phase 2 Report**  
**6.0 Slope Stability Analysis**

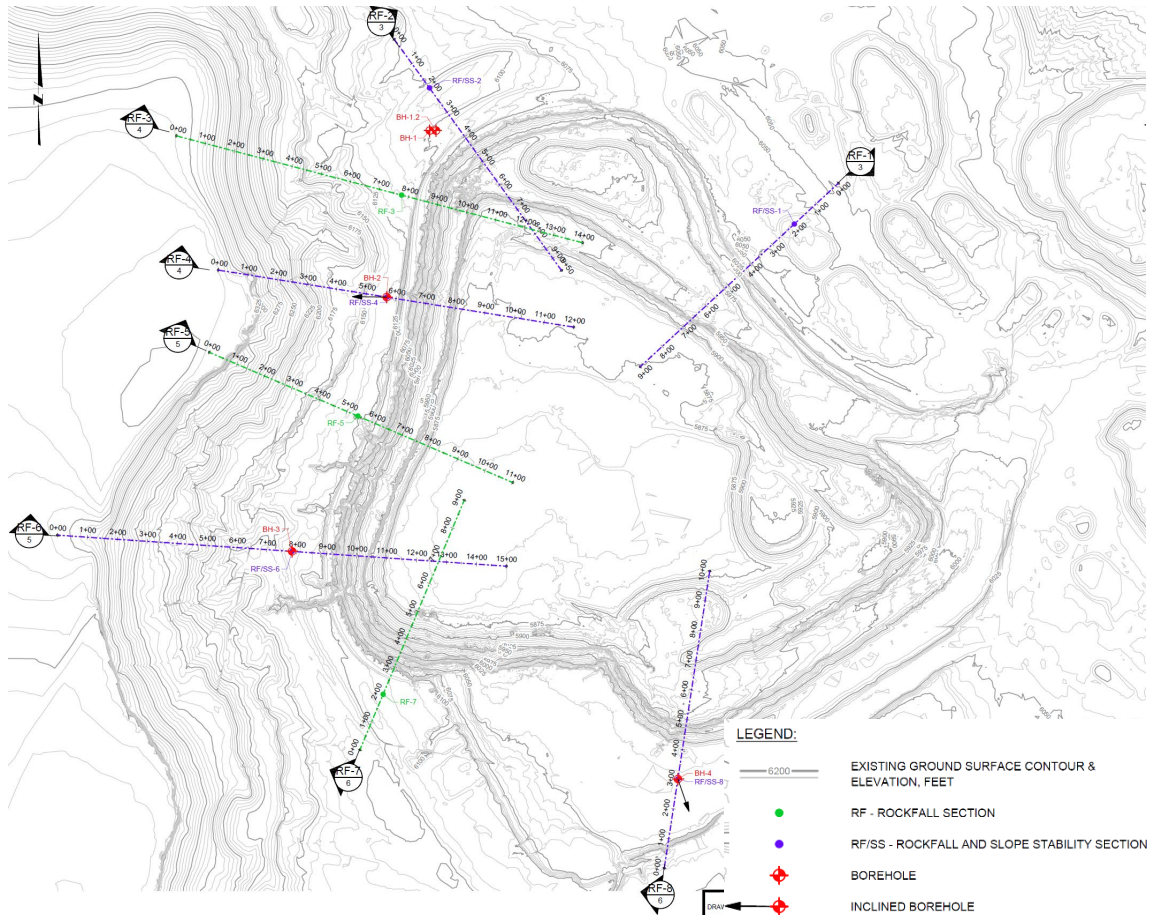


**Figure 10: Pit 1 Highwall Stability and Rockfall Sections**

Limit equilibrium analysis was carried out using the software Slide2 from Rocscience Inc. (Rocscience, 2020). The analysis considered both circular and non-circular failure types. The GLE Morgenstern Price calculation method was used. Non-circular failure surfaces were optimized using the Slide2 Cuckoo search algorithm.

The FOS was calculated for the various models and compared with the selected FOS acceptance criteria. The selected FOS acceptance criteria used for these analyses are 1.3 for static conditions, 1.0 for pseudo-static conditions, and 1.1 for shallow bench failure based on Guidelines for Open Pit Design assuming a low consequence of failure Pit (Read, 2019 [Table 9.9]).



## **6.5 Methodology**

### **6.5.1 Slope Parameters**

Five sections along the pit highwall were used for the slope stability analysis. Representative sections were selected to represent the highest and steepest slopes along the west, north, east, and south highwalls. Four of the sections coincided with borehole locations and a fifth was included along the northeast highwall (Section 1). The sections were taken from the available ground surface Lidar data for the pit. Stability was analyzed for the current highwall slopes and pit floor elevations. Approximate locations of the sections are shown in Figure 10.

### **6.5.2 Rock Parameters**

All rock formations except the Mancos Shale were modeled using Hoek-Brown Generalized failure criterion assuming the rock mass shear strength is generally isotropic.

The Mancos Shale was modeled assuming anisotropic rock mass characteristics. The Snowden Method was used, applying anisotropic linear strength formulas to account for different strengths parallel and perpendicular to the bedding. Bedding and rock mass shear strength functions were determined with RSDData and imported into Slide2.

The angle of anisotropy was selected as 0 degrees (horizontal) based on the observed near horizontal bedding planes in the rock core and downhole televiewer surveys. Bedding shear strength parameters were applied to slip surfaces within  $\pm 5$  degrees of the bedding orientation. A  $\pm 30$ -degree transition zone between rock mass strength and bedding strength was applied.

Table 11 presents the average Hoek-Brown material parameters input into RSDData. Table 8 in Section 5.2.5 presents the average Barton Bandis properties input for the Mancos Shale discontinuities.



**St. Anthony Mine: Pit 1 Highwall Stability – Phase 2 Report**  
**6.0 Slope Stability Analysis**

**Table 11: Hoek-Brown Average Material Parameters**

Hoek-Brown Parameters	Rock Unit			
	Mancos Shale	Mancos Siltstone/Sandstone	Dakota Sandstone	Jackpile Sandstone
Uniaxial compressive strength (UCS) (ksf)	636	816	1237	490
GSI	35	45	45	55
$m_i^1$	6	6	17	17
Disturbance factor (D) <sup>2</sup>	1	1	1	1
Elastic modulus (ksf)	101,524	129,114	336,965	119,527

<sup>1</sup>  $m_i$  constants were selected using Table 4.5 in Rock Slope Engineering (Wyllie, 2018)

<sup>2</sup> A disturbance factor (D) of 1 was applied to a 45ft zone at the edge of each section in the stability model

**Weak Layers**

Weak zones for each borehole were located primarily in the upper portion of the Mancos Shale. Weak layers, greater than 2 ft and less than 10 ft thick noted on borehole logs as soft shale zones, voids, or zones with low core recovery were applied to stability sections SS-2, SS-4, and SS-6 using the weak layer tool in Slide2. Lower bound compressive strengths, one standard deviation below the average, and GSI values selected as described in section 5.2.2 were applied to the weak layers. Weak layers in the Mancos Shale were modeled with anisotropic rock mass characteristics using the Snowden Method, as described in this section.

Table 12 presents the lower bound Hoek-Brown parameters input into RSDData to model weak layers. Table 8 in Section 5.2.5 presents the lower bound Barton Bandis properties input for the Mancos Shale discontinuities.

**Table 12: Lower Bound Hoek-Brown Parameters**

Hoek-Brown Parameters	Rock Unit			
	Mancos Shale	Mancos Siltstone/Sandstone	Dakota Sandstone	Jackpile Sandstone
Uniaxial compressive strength (UCS) (ksf)	429	572	661	329
GSI	30	35	40	50
$m_i^1$	6	6	17	17
Disturbance factor (D) <sup>2</sup>	1	1	1	1
Elastic modulus (ksf) <sup>3</sup>	101,524	129,114	336,965	119,527

<sup>1</sup>  $m_i$  constants were selected using Table 4.5 in Rock Slope Engineering (Wyllie, 2018) this value remains the same as average values for weak layers.

<sup>2</sup> A disturbance factor (D) of 1 was applied to a 45-ft zone at the edge of each section in the stability model.

<sup>3</sup> The average elastic modulus was used for weak layers



### **Blast Damage**

Blast damage is a result of uncontrolled blasting techniques to excavate and create the pit slope wall. The blast induced fractures are created as the explosion penetrates the slope walls. The blast induced fractures extend behind the pit face as a blast damage zone (D). The depth of penetration and degree of fracturing will depend on the blast methods used. No specific details are available on excavation and blasting techniques used at the site. Using the Hoek-Brown criterion for surface mining (Hoek, 2000), we have assumed production blasts, with no control but blasting to an open face. The height of the benches was estimated from visual interpretation of the drone images and LiDAR sections to be approximately 30 ft. The analysis has assumed a uniform blast damage zone depth of approximately 45 ft (1.5 times the estimated bench height) from the existing pit slope face into the rock mass (Hoek, 2000). A blast damage factor of  $D = 1.0$  (Hoek, 2000) was applied to the Hoek-Brown material properties within this zone. The visual GSI value used in the model accounts for some of the blast damage observed visually on the surface of the highwall. The addition of the blast damage factor adds a degree of conservatism and may account for additional damage, stress release and weathering along the edge of the highwall.

### **6.5.3 Groundwater**

Groundwater levels along the cross-sections were estimated using INTERA contours within the Jackpile formation (INTERA, 2015) and were assumed to be relatively flat near the center of the pit, increasing gradually in elevation along the highwall away from the pit.

### **6.5.4 Seismic Parameters**

Half of the 10,000-year PGA was applied to each stability section as a pseudo-static load (Abramson L.W., 2000). The location specific PGA was 0.27g (see Section 2.3), resulting in a pseudo-static horizontal load applied in the model of 0.14g.

### **6.5.5 Geometric Search Constraints**

In Slide2, circular and non-circular cuckoo search methods were used to search for slip surfaces within set entry/exit point extents along the slope. Non-circular failure surfaces were optimized to calculate the lowest possible factor of safety for the critical failure surface. The GLE/Morgenstern Price method was used to calculate interslice forces for the FOS. For the global stability assessment, entry / exit points were set to force failure through a minimum of two benches and the failure surface area was set to a minimum of 100 ft<sup>2</sup>. For a shallow stability assessment, slip surface entry / exit points extents were set to confine the failure surface within a smaller portion of the slope and the minimum failure surface area was set to 50 ft<sup>2</sup>, allowing failure through individual benches.



## 6.6 Stability Analysis Results

### 6.6.1 Static Stability

FOS results for global failure through a minimum of two benches were above the FOS target criteria of 1.3. Sections SS-1, SS-2 and SS-8 along the northern and southern portions of the highwall had the highest static FOS results, generally greater than 2. The tallest and steepest sections, SS-4 and SS-6 along the western highwall, had the lowest static FOS results in the range of 1.5 to 1.7. Results of the global static stability analyses are shown in Table 13.

**Table 13: Global Static FOS Results**

Sections	Circular Failure Surfaces		Non-Circular Failure Surfaces	
	Without Weak Layers	With Weak Layers	Without Weak Layers	With Weak Layers
SS-1	5.0	-	3.0	-
SS-2	2.3	2.3	2.0	2.0
SS-4	1.5	1.5	1.4	1.4
SS-6	1.9	1.9	1.6	1.6
SS-8	2.0	-	1.9	-

Note: Weak layers were determined from borehole log data, sections without weak zones did not have available borehole data or did not contain weak layers in the borehole data.

For each section, the failure surface with the lowest FOS was generally located within the assumed 45 ft blast damage zone near the edge of the highwall, see Figure 11. FOS beyond the disturbance zone were generally greater than 2.



**St. Anthony Mine: Pit 1 Highwall Stability – Phase 2 Report**  
**6.0 Slope Stability Analysis**

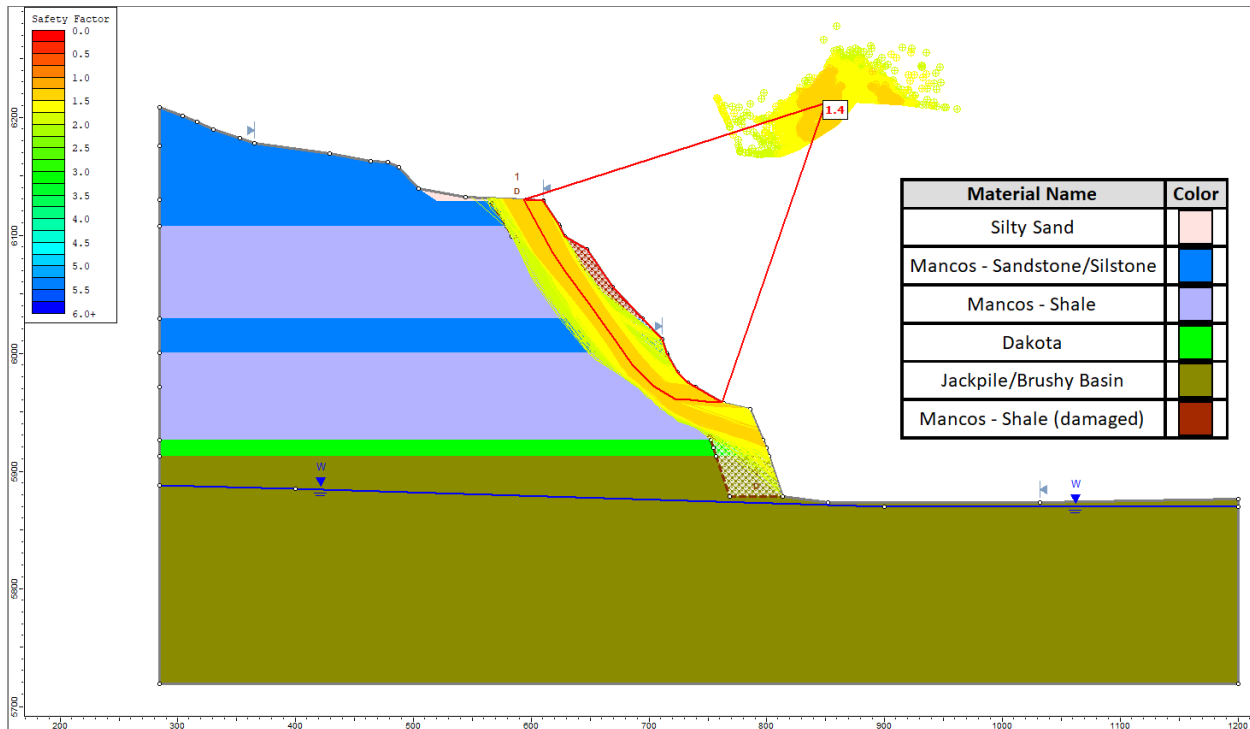


**Figure 11: SS-4 with Weak Zones Showing All Non-Circular Surfaces with FOS < 2**

The results indicate the assumed blast damage zone has a significant impact on stability results. Failure surfaces generally occurred within the Mancos formation due to its lower rock mass strength properties. Global failure surfaces generally did not occur through the weak zones due to their locations along the highwall.

Non-circular failure surfaces passed through the horizontal bedding planes of the Mancos Shale for some sections. This reduced the FOS compared to circular failure surfaces; however, the FOS still met target criteria. Weak zones within the Jackpile formation are below the critical failure surfaces and did not result in failure surfaces with lower FOS. The assumed groundwater level is below any failure surfaces and does not impact the FOS. The static stability results indicate that the slopes in Pit 1 meet the target FOS criteria of 1.3 for rock mass failures larger than 2 benches.

**6.6.2 Pseudo-Static**

Results of the pseudo-static analysis met the target FOS criteria of 1.0. Similar to the static results, SS-1 and SS-8 had the highest FOS results and SS-4 and SS-6 the lowest. Results of the pseudo-static analyses are shown in Table 14.



**St. Anthony Mine: Pit 1 Highwall Stability – Phase 2 Report**  
**6.0 Slope Stability Analysis**

**Table 14: Global Pseudo-Static FOS Results**

Sections	Circular Failure Surfaces		Non-Circular Failure Surfaces	
	Without Weak Layers	With Weak Layers	Without Weak Layers	With Weak Layers
SS-1	3.8	-	2.5	-
SS-2	1.9	1.9	1.7	1.7
SS-4	1.3	1.3	1.2	1.1
SS-6	1.6	1.6	1.4	1.4
SS-8	1.6	-	1.5	-

Note: Weak layers were determined from borehole log data, sections without weak zones did not have available borehole data or did not contain weak layers in the borehole data.

**6.6.3 Shallow Static Stability**

Shallow static failure results met the target FOS criteria of 1.1. See the results in Table 15.

**Table 15: Surficial Static FOS Results**

Sections	Circular Failure Surfaces		Non-Circular Failure Surfaces	
	Without Weak Layers	With Weak Layers	Without Weak Layers	With Weak Layers
SS-1	3.2	-	3.1	-
SS-2	1.7	1.6	1.7	1.6
SS-4	1.3	1.3	1.3	1.3
SS-6	1.3	1.3	1.3	1.3
SS-8	2.3	-	2.3	-

Note: Weak layers were determined from borehole log data, sections without weak zones did not have available borehole data or did not contain weak layers in the borehole data.

The steepest and tallest highwall sections, with the lowest factors of safety among those analyzed are located along the west side of the Pit. The shorter and less steep highwall sections along the north and south portions of the pit generally resulted in factors of safety greater than 2. Surficial FOS results were generally less than the global FOS results.

The assumed 45-ft blast damage zone had a significant impact on the stability of surficial materials. Although factors of safety remained above 1.3, static surficial failures had lower factors of safety than global failures for both static and pseudo-static conditions.

Most shallow failures analyzed occurred within the upper layer of the Mancos Shale, due to the weak rock mass. Weak zones within the upper Mancos Shale layer controlled the failure surfaces; however, did not significantly reduce the resulting shallow factors of safety.



**St. Anthony Mine: Pit 1 Highwall Stability – Phase 2 Report**  
**6.0 Slope Stability Analysis**

Small overhangs and partially or fully detached rocks observed in the Mancos formation along the highwall are not captured in this stability analysis but could be subject to instability. Laboratory durability test results indicated the near surface Mancos is highly susceptible to weathering over time in wet-dry and freeze-thaw conditions. Although the blast and drilling damage zone significantly impacts stability results, it does not account for future erosion or surficial weathering. Future conditions and small-scale overhang features were not modeled but could cause smaller scale surficial rockfalls or sloughing failures. Based on these observations, scaling of surficial weathered material and overhanging rocks is recommended in Section 8.0.

In general, the surficial stability results did not indicate necessary slope changes due to local bench failure. Visible observations of the highwall conditions indicate removal of loose or overhanging surficial materials from the Mancos formation may be necessary to prevent rockfall and small surficial failures. These actions will be evaluated in the 90% CCOP.



## **7.0 ROCKFALL ANALYSIS**

Stantec undertook a preliminary rockfall analysis on Pit 1 during Phase 1 of the highwall assessment (as mentioned in Section 1.2), which was based on visual observations of rockfall coupled with LiDAR models and photogrammetry to identify existing blocks and rockfall distances from the toe of the slope. Results of this preliminary analysis suggested the need for a hazard exclusion zone and/or hazard control solution to mitigate rockfall as part of the final closure design to protect workers in the pit bottom. Beyond construction for closure activities, rockfall hazard will be further mitigated by restricted access into the bottom of the pit. Limited data was obtained during Phase 1 that would allow for an initial assessment of design solutions, so a more quantitative approach was suggested as a follow-up analysis for Phase 2, building on the preliminary data collected for Pit 1. A detailed modelling approach was recommended to better assess the trajectories and impact forces expected, which will allow for future design of mitigation measures in the pit bottom as part of the Pit 1 closure plan.

The supplemental rockfall analysis for Phase 2 was undertaken using eight sections (RF-1 through RF-8) distributed around the Pit 1 highwall (shown above in Figure 10). The sections were assessed in their existing state, and sections RF-4 through RF-7 were also ran with the proposed pit backfill and a 2-meter waste rock berm design for comparison. Five out of the eight rockfall sections, shown on Figure 10 and discussed in Section 7.1, were also used for the global slope stability analysis for correlation including RF-1, RF-2, RF-4, RF-6, and RF-8.

The following are assumptions and limitations associated with the rockfall analysis that must be considered.

- Predicting rockfall triggering and occurrence is dependent on many variables that are not realistically quantifiable (i.e., erosion, degree of weathering or alteration, meteorological and hydrological conditions, rock quality, etc.), and thus the rockfall models can only estimate the rockfall.
- Rockfall initiation points were selected based on engineering judgement of the most likely hazard elevations along the highwall. Significant future erosion, subsurface anomalies, and other factors may contribute to additional areas where rockfall is more likely to occur; this is beyond Stantec's ability to predict.
- Highwall surfaces are assumed to be semi-continuous in the models to assign average properties to them, which are used to predict rock movement across them.
- The rockfall model does not simulate rocks being broken, as the rocks impact the slope while failing, which is likely to occur with sedimentary rocks that are weathered or have a tight joint spacing.
- The parameters used in the Rocfall3 model were selected by Stantec based on our site observations, a literature review of parameter inputs used on comparable sites, and assumptions of the velocity and height rocks will be released when excavated. Some variability should be expected between the model's outputs and the true runout path of



seeders. Further, there is inherent aleatory and epistemic uncertainty associated with modeling rockfalls with a numerical software. Model results should be considered indicative of rockfall behavior and characteristics on the slope, and not a predictor of actual rockfall.

The rockfall modelling approach and discussion of the analyses are described in detail in the following subsections.

## **7.1 Methodology**

Software chosen for this analysis is from the same software suite as the stability analysis completed for the pit but using the program Rocfall version 6.0 from Rocscience (Rocscience, 2018). The rockfall analysis incorporates the Rigid Body Method analysis. Advantages of this method are more realistic characteristics and material properties assigned to both the rock-blocks and the pit slopes themselves. Typical rockfall modelling approaches used by various industries (including mining) to understand potential risks use a simplified version of Rigid Body Mechanical Theory to simulate rockfall behavior as either a Rigid Body approach, Lump Mass approach, or hybrid between these two (Ashayer, 2007). Using Discrete Element Modelling (DEM) program such as Rocscience to apply a Rigid Body analysis to the rockfall evaluation is considered a more comprehensive analysis approach (Wyllie, 2015). Surface topography data from the Phase 1 LiDAR survey was used to generate the 2-dimensional surfaces input into the rockfall models along each section. Stantec modelled sections RF-1 and RF-4 first varying the rockfall parameters to calibrate our model inputs to real world observations from Phase 1 in Pit 1.

## **7.2 Rockfall Parameters**

During the Phase 1 analysis, Stantec collected field observation data through photographs and manual measurements of detached rock blocks primarily from both Mancos and Dakota formations found on the pit floor and observed on the highwalls. These measurements and observations were used to inform our modelling approach for rock sizing and shapes that occur at the site. Supplemental information on realistic unit weights for rock block materials was derived from the Phase 2 laboratory testing efforts on the four rock coring holes completed for this scope of work. Multiple rock sizes were modelled at the varying seeder heights simultaneously for certain locations where visual observations and drilling fracture frequency data supported this, to represent a range of rockfalls that have been observed throughout the pit. Upper Sandstone Rockfall Blocks were used in conjunction with Average Rockfall Blocks at benches observed to have higher competency and observable large boulders present (such as the upper pit edge seeder location and upslope features such as the west-Mesa adjoining Pit 1). Lower Siltstone blocks were similarly placed at certain seeders, exclusively for the lowest observable bench at each section and alongside Average Rockfall Block's for seeders near the bottom. The input parameters for the rockfall material assumed for the analysis are shown here in Table 16.



**St. Anthony Mine: Pit 1 Highwall Stability – Phase 2 Report**  
**7.0 Rockfall Analysis**

**Table 16: Rockfall Model Input Parameters**

Parameter	Unit Weight	Mass (Approx. Size)	Shape	Seeder Location Initial Velocity (ft/s)	Source/Comments
Detached Upper Sandstone Rockfall Block	140 lb/ft <sup>3</sup>	80,000 lb (15ft x 7.5ft x 5ft)	Polygon Rectangles with side ratios of 1:2 and 2:3 Super Ellipses with elongation ratio of 2:3	0.75	Stantec visual observation, upper mesa and highwall crest
Average Rockfall Block in Talus	140 lb/ft <sup>3</sup>	3,400 lb (4ft x 3ft x 2ft)	Polygon Rectangles with side ratios of 2:3 and 5:6	0.5	Stantec visual observation, multiple benches, and talus/scree piles near pit toe
Lower Siltstone Eroded Block	140 lb/ft <sup>3</sup>	5,000 lb (4ft x 4ft x 2ft)	Hexagon Rhombus	0.5	Stantec visual observation

### 7.3 Slope Parameters

The slope materials used in the rockfall modelling to represent the pit surface were selected based on visual observations of slope features present during our Phase 1 assessment along with geological formations encountered during the 2021-22 drilling investigation at BH-1 through BH-4 around the pit highwall. Material parameters were selected based on literature (Wyllie, 2014 and Rocscience 2021) and our experience on similar projects. The values of the parameters for each adopted slope material derived from mean values provided in literature for the specific site conditions are summarized in Table 17.



**St. Anthony Mine: Pit 1 Highwall Stability – Phase 2 Report**  
**7.0 Rockfall Analysis**

**Table 17: Rockfall Analysis – Input Parameters Slope Material**

Geological Formation	Color (see Fig 2X)	Restitution		Friction		Slope Roughness (ft)	
		Normal	Tangential	Dynamic	Rolling	Spacing	Amplitude
Bedrock Face		0.35	0.8	0.63	0.3	-	-
Talus		0.32	0.76	0.55	0.25	-	-
Compacted Haul Road		0.38	0.81	0.63	0.2	-	-
Waste/Fill Material		0.29	0.68	0.56	0.35	-	-
Vegetated Soil Slope		0.3	0.73	0.6	0.3	-	-
Weak Shales		0.28	0.71	0.46	0.15	3.28	0.33
Jackpile Sands		0.34	0.72	0.62	0.4	-	-

The parameters for slope properties are determined from the velocity changes of the rockfall as a result of deformation and friction at the impact surface. The velocity of the rockfall is separated into normal (perpendicular to the slope) and tangential (parallel to the slope); the plasticity of the surface material determines the energy dissipation normal to the surface, while the surface friction determines the reduction in motion parallel to the surface. The coefficient of restitution is a function of the change in velocities before and after contact at the slope face. The friction parameter is determined by the changes in rotational and translational velocity at the slope face contact.

An example of the general slope models showing the various material types assumed is shown in Figure 12.



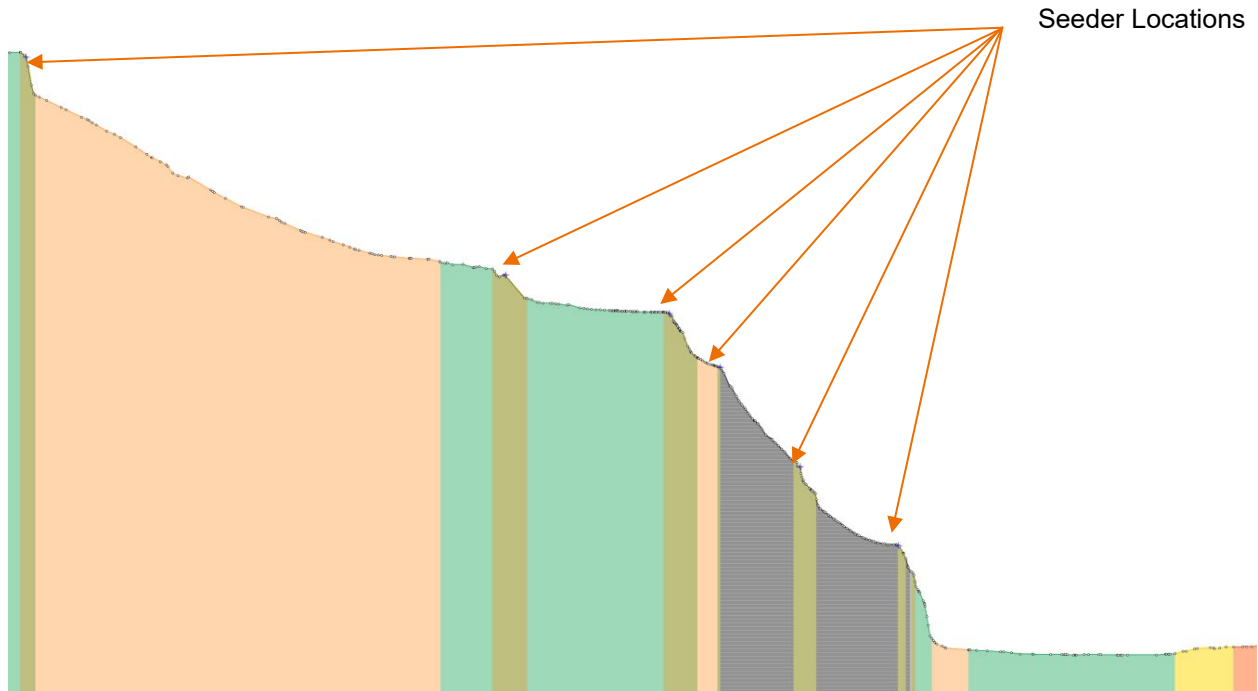


**Figure 12: Example of Slope Model – Section 4 (Calibration Run)**

The analysis was carried out using several seeder locations (i.e., falling rock initiation locations near the slope with the greatest slope change) from where rockfall has greater potential to originate. A combination of three to five seeder locations were selected across each section depending on intact benches, presence of upper mesa or waste rock piles, or unique pit geometry affecting the number of locations. Generally, a seeder was placed in the Dakota and Mancos formations near the crest of the highwall, mid-slope at a prominent bench with observed overhang, and at a lower bench near the base of the wall on all slope sections. Lowest seeder locations in east pit wall sections RF-1 and RF-2 were placed in what is estimated to be near the top of the Jackpile formation to assess potential roadway disturbance induced rockfalls that are not anticipated to make up a significant volume of rockfall hazard for the highwall. Seeder locations along the slope were assigned rock blocks to fall depending on location along the slope and were assigned 500 rock simulations for the upper large blocks or 1000 rock simulations for the rest of the seeders. Locations were selected at each section using visual observations of outcrops during the field investigation, in addition to photographs collected of the pit highwall during the Phase 1 analysis.

### 7.3.1 Modified Pit Slope Alternatives

To guide our recommendations on closure design regarding the rockfall analyses, Stantec also generated modified slope sections for RF-4 through RF-7. This was not part of our original Phase 2 scope but was performed as a value-add to better inform the final closure design.



**St. Anthony Mine: Pit 1 Highwall Stability – Phase 2 Report**  
**7.0 Rockfall Analysis**

For these supplemental analyses, Stantec considered the following adjustments to assess relative rockfall hazard improvement achieved after final construction using a variety of mitigation techniques.

- Raising the Pit 1 floor elevation to the preliminary closure elevation currently presented in the 30% CCOP.
- Placement of a simple berm at 20 to 100 feet from the highwall face.
- Toe of slope talus material removal.
- Bench cleaning (removal of loose material from the benches of the Dakota and Mancos formations).

The scenarios are described below with the results and were used to develop recommendations.

**7.4 Results**

The rockfall analysis results for the eight slope sections are summarized in Table 18 with model outputs and summary graphs provided in Appendix L. Collector nodes were placed approximately 20 to 50 ft out from the toe of the highwall slope (not the toe of the highwall face) to gather data on rock energy within potential work areas and look at bounce heights. Distances for rockfall trajectories measured from the highwall face were also recorded.

**Table 18: Summary of Rockfall Analysis Results**

<b>Rockfall Model Results</b>	<b>RF-1</b>	<b>RF-2</b>	<b>RF-3</b>	<b>RF-4</b>	<b>RF-5</b>	<b>RF-6</b>	<b>RF-7</b>	<b>RF-8</b>
Collector distance from highwall-toe (ft)	25	10	50	40	22	40	22	35
Percentage of retention (all seeder locations) (%)	70	80	99.9	41	64	78	87	35
Percentage of rockfall behind seeder location (%)	100	85	100	66	83	97	93	100
Maximum bounce height (ft)	-	2.03	-	13.74	15.41	20.88	20.61	5.84
Average collector impact energy (ft-lbs)	-	4 x 10 <sup>3</sup>	-	6 x 10 <sup>4</sup>	5 x 10 <sup>4</sup>	8 x 10 <sup>5</sup>	9 x 10 <sup>5</sup>	2 x 10 <sup>5</sup>
Maximum trajectory runout (ft)	36	18	25	83	75	105	90	41



## St. Anthony Mine: Pit 1 Highwall Stability – Phase 2 Report

### 7.0 Rockfall Analysis

The results of the rockfall analysis for Pit 1 indicate great variability in rockfall retention, runouts, and potential bounce heights for all seeder locations considered per section. Rockfall retention varied from as little as 35% up to 99.9%, runouts ranged from 18 to 105 ft, and bounce heights at strategic locations from the highwall toe range from 2 ft to over 20 ft. The highest energy encountered at a collector location was around  $9 \times 10^5$  ft-lb from a mid-slope originating rock.

#### *Section RF-1*

This section is on the northeast portion of the pit where the topography dips and the total height is less than a majority of the other sections. Additionally, Section RF-1 has a wide haul road mid-slope to act as a catch berm for most of the potential rockfall. Our analysis of RF-1 resulted in minimal runout from the toe of slope, with all the rockfall making it into the pit bottom (30% of the total rockfalls triggered), originating downslope of the haul road. Furthermore, most of the rockfall originating near the crest was caught on catch benches immediately below the seeder locations and none was shown to make it onto the main access road leading to the bottom of the pit necessary to be maintained for closure activities and pit access. Rockfall making it into the bottom of the pit at this location was rolling and no longer travelling vertically after 20 ft out from the toe of the highwall.

#### *Section RF-2*

Our analysis for RF-2 showed only 20% of the modeled rocks reaching the toes of the slope and a maximum runout from the rockfall into the pit of just 18 ft. A wide bench mid-slope remains intact which serves as a good protection for most of the rockfall hazards likely to occur at this section. Impact energies on the collector placed 10 feet from the toe are still significant, reaching  $4 \times 10^3$  ft-lb, but a maximum bounce height of 2 ft was observed for this attributing to most of the rocks rolling instead of bouncing/falling near the toe.

#### *Section RF-3*

Moving towards the northwest corner of the pit, the existing haul road shifts away from the pit wall and a large bench above (mostly full of debris) exists. The piled debris plays a large role at this portion of the pit in preventing rockfall from entering the pit bottom, with the model estimating less than 1/10th of a percent reaching the toe of the highwall. Runout from rolling rocks is approximately 25 ft onto the existing haul road, meaning none of the rocks reached the inside edge of the haul road at this location and would likely not be able to continue into the bottom of the pit. These results may vary short distances from the selected section as the lower pit geometry changes.

#### *Section RF-4*

This area of the pit was a high priority for initial calibration and overall analysis based on visual observations of large, detached blocks on the pit floor, ongoing highwall channel erosion, and the presence of an upper mesa with gradual slope leading down to the pit crest. We placed a seeder at 40 ft from the toe for this analysis which is approximately 15 ft into the haul road. This section had 59% of the modeled rockfall make it all the way to the pit floor from all seeder locations, except for the upper mesa rockfalls which had no rocks make it to the crest of the pit at all. Total



## St. Anthony Mine: Pit 1 Highwall Stability – Phase 2 Report

### 7.0 Rockfall Analysis

runout produced was 83 ft from the toe of the slope, with rocks bouncing on average of 2.5 ft above grade and up to 13.7 ft at a distance of 40 ft from the toe. Maximum energy observed at rocks travelling through the middle of the haul road were  $5.8 \times 10^4$  ft-lb. Results at this section show a significant amount of rocks falling (as opposed to primarily rolling) a significant distance from the toe of the highwall face, as well at distances exceeding 40 ft.

#### *Section RF-5*

Along the west highwall in the north-central portion, the slope geometry is still steep but shows an increase in talus material accumulated on benches resulting in 36% of modeled rockfalls making their way to the pit floor with a maximum runout distance of 75 feet. The rockfalls originating from the crest at this location did not make it to the pit floor, nor did any of the upper mesa rockfalls. A seeder placed just 22 feet from the toe of the slope (approximately 60 feet from the nearest vertical highwall face) at this location in the flat pit floor showed average bounce heights around 3.1 feet and reaching 15.4 feet on the high end. Energy observed this close to the slope reached a maximum of  $4.6 \times 10^4$  ft-lbs, with most observed rockfall presenting a rolling hazard beyond the collector distance.

#### *Section RF-6*

Moving to the south-central portion of the west highwall, we saw the greatest runout distance at this location, at 105 ft, from 22% of the cumulative modeled rockfall making its way to the pit floor. A collector distance similar to RF-4 of 40 ft was used at this location which showed average bounce heights of 6.7 ft and over 20 ft for a maximum. Maximum energy at this distance from rocks moving past the collector reached  $7.5 \times 10^5$  ft-lb. Larger rocks from above had a tendency to bounce off the slope and fall farther out from the face compared to smaller and average rocks, originating lower down the highwall which generally rolled with minimal bounce.

#### *Section RF-7*

Near the southwest corner of Pit 1, a much higher degree of erosion is present on the slopes resulting in a semi-continuous slope near the angle of repose for talus material that has filled the benches from the crest down to the toe. A pile of debris (talus and eroded soils) has also accumulated near the toe at this location and partially vegetated which benefits this slope in catching rockfall, with only 13% of total modeled rockfall making it all the way to the pit floor. Runout distances reach 90 ft at this location, and a collector placed at a similar distance as RF-5 (22 ft) shows average bounce heights of 7.5 ft and up to over 20 ft. Maximum rock energy observed at the collector was close to  $9 \times 10^5$  ft-lb with rocks observed bouncing many times near slope and generally bouncing all the way out near the final runout trajectory.

#### *Section RF-8*

Section RF-8 on the southeast portion of the pit includes a large upper bench below a mesa, followed by a wide haul road mid-slope with talus covering the upslope portion and stockpiled waste rock / fill materials downslope of the haul road. A collector was placed just to the inside of the haul road approximately 35 ft from the slope break, which showed average bounce heights of



## St. Anthony Mine: Pit 1 Highwall Stability – Phase 2 Report

### 7.0 Rockfall Analysis

5.1 ft up to a maximum of 5.8 ft, and a maximum runout from the toe (above the haul road) at 41 ft. Impact energies reached  $1.9 \times 10^5$  ft-lb.

#### 7.4.1 Modified Pit Slope – Partial Backfill

Rockfall section RF-4 was run with a modified Pit 1 floor elevation to approximately 5,890 ft AMSL, approximately the proposed final design elevation currently in the 30%CCOP. For this simulation, no other modifications to the slope were made. The change in the Pit 1 floor elevation alone did not have a major impact on the maximum runout distance from the toe which still exceeded 80 ft but did result in higher bounce values for initial impacts and slightly decreased volume of runout to this distance in total rockfalls simulated. Rocks were modeled to be falling before bouncing on the pit floor more than 45 ft from the highwall face near the toe. From this simulation, we anticipate the proposed pit backfill elevation will slightly reduce rockfall runout and bounce hazards in the pit floor because of the tendency to lose energy quicker with vertical bounces as opposed to more horizontal trajectories that allow for more energy retained during runout in the current slope configuration model. This assumption generally holds true regardless of the pit backfill elevation, so changes on the order of less than 10 ft during final design to the pit floor elevation are not anticipated to significantly impact mitigation measures implemented during construction.

#### 7.4.2 Modified Pit Slope – Berms, Backfill, and Benches

To further analyze potential changes to the rockfall results after closure construction, we also modified the slopes of RF-4 through RF-7 to accommodate a catch bench in a likely location (see Figure 13 below), added a 6-foot-tall berm near the toe, and incorporated the design pit floor elevation mentioned above. For sections RF-4 and RF-5, fall distance was decreased to less than 35 ft with more than 99% of the modeled rockfall being stopped by catch benches at elevations 5,955 ft and 5,897 ft AMSL, respectively or by the berm on the regraded floor 30 ft or 20 ft from the highwall face, respectively. For RF-6, a bench at elevation 5,955 and 6-foot berm 45 ft out from the highwall face captured a large percentage of modeled rockfall and rocks bouncing but was not sufficient to capture the full trajectory of over 100 ft on the pit bottom. For section RF-7, a lower regraded bench near the toe of the final pit bottom and a berm at 100 ft from the highwall face (45 ft from the toe of slope) captured more than 90% of the rockfall with a few higher bouncing rocks reaching close to 100 ft of runout from the toe.





Figure 13: Simulated Rockfall Bench Cleaning Locations

## 7.5 Discussion

Our rockfall analysis produced representative results for observed rockfall behavior at the site and furthered the understanding on how the rockfall hazard may continue through greater runout trajectories and high energy rocks impacting the pit floor. The modelling also showed variability around the pit, highlighting the most hazardous portion of Pit 1 as the southwest side of the highwall and eliminating several areas as high hazard potential locations.

### 7.5.1 Existing State – Critical Risks

Currently, the greatest risk to workers in the pit bottom posed by rockfall, exists at sections RF-4 through RF-7, with RF-6 showing the largest potential for presenting a risk to personnel and equipment in the pit bottom. The energies observed for these sections exceed the testing standards for heavy duty machinery on cab protection (ISO 3449:2005, Level 2) by 10x to over 100x the impact protection loads the equipment is designed for. With rocks travelling 75 to over 100 ft from the toe of the working slopes in the existing condition, these areas present a significant hazard to personnel working in the pit within approximately 150 ft of the highwall on the west side of Pit 1.



## St. Anthony Mine: Pit 1 Highwall Stability – Phase 2 Report

### 7.0 Rockfall Analysis

The accumulation of talus material on benches and near the toe of the slope has also shown in the models to increase the distance from the highwall that rocks can travel along sections RF-6 and RF-7. These models show that despite the decreased vertical energy from upper falling rocks by having more gradual slopes, a different hazard is created through bouncing material that can reach significant heights and travel 90 to 105 ft from the toe.

In the current condition, the upper mesa rocks are unlikely to present a common hazard around, or in, the bottom of the pit. Additionally, the existing haul roads on the northeast and south portions of the pit have a favorable effect and reduce the potential for rockfall to occur near the middle of the roads. Section RF-4 shows a potential for runout mid-way into the haul road, but with bounce heights that are on average less than half the height of a standard pickup truck that would be travelling these roads.

#### 7.5.2 Improved State – Mitigation Strategy

A proposed mitigation analysis will be conducted with the 90% CCOP (further described in the recommendations below), the higher hazard areas near the southern portion of the west highwall remain a key area for mitigation efforts. Placement of berms approximately 20 ft from the highwall out to 100 ft moving south along the west highwall, are anticipated to be a viable long-term solution to capture a significant portion of rockfall that may continue to occur post-closure. Current closure plans restrict public access to the pit, but post-closure O&M activities necessitating worker access into the pit shall be subject to exclusion zone distances specified in the O&M manual. During construction, exclusion zones for workers will need to be specified according to construction sequence and should be marked with signage throughout the closure process. Cleaning the existing benches using a specialty contractor to remove excess material in a manner they deem appropriate is also considered to be a key component to decreasing the amount of rockfall that can occur past the toe of slope. A conceptual approach showing rockfall berm placement is shown below in Figure 14. Current stormwater management design considerations for the Pit 1 cover could be incorporated through gaps in the berm design for closure, to allow stormwater flow back to the center of the pit.



St. Anthony Mine: Pit 1 Highwall Stability – Phase 2 Report  
7.0 Rockfall Analysis

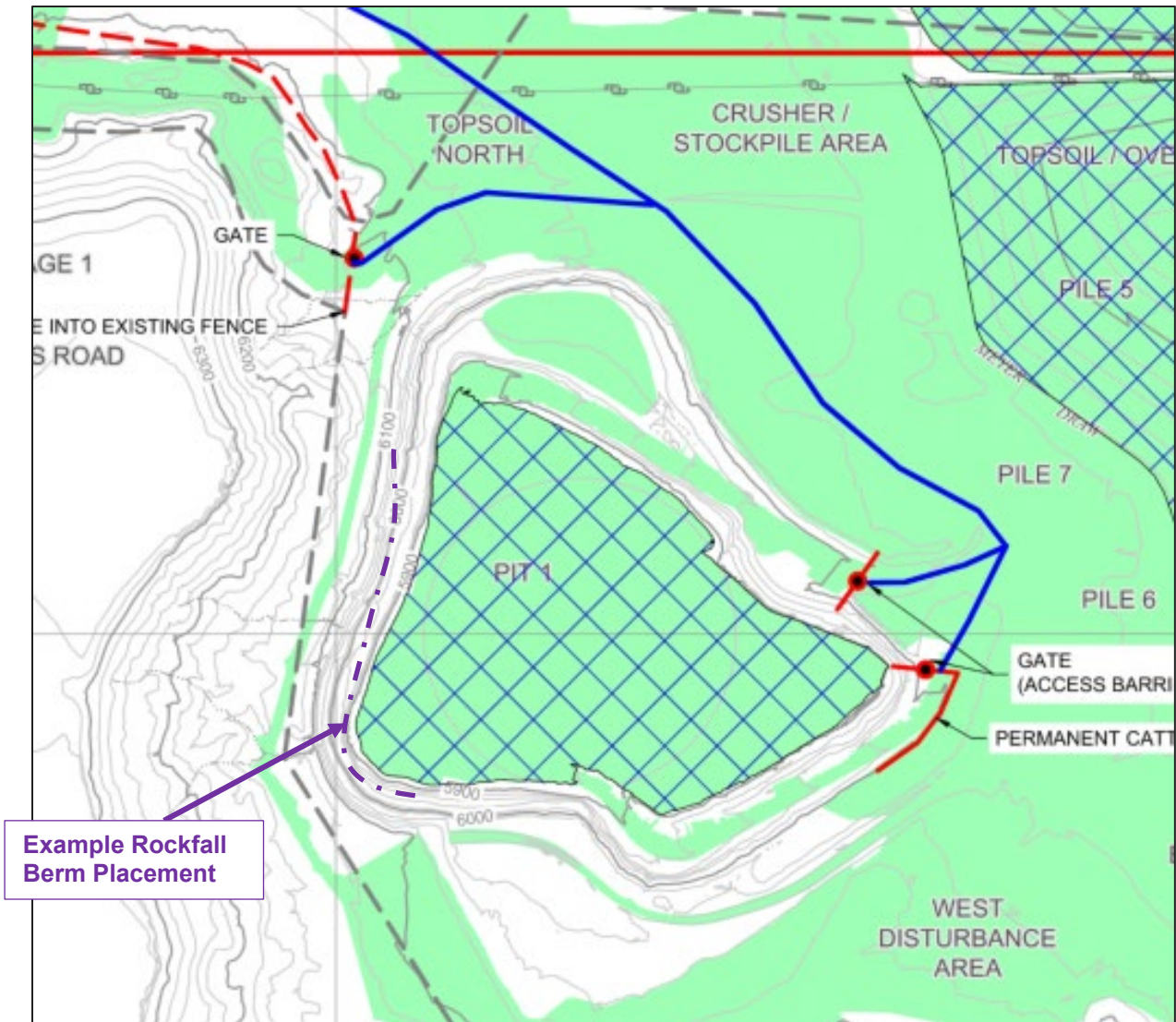


Figure 14: Conceptual Berm Placement



## **8.0 CONCLUSIONS AND RECOMMENDATIONS**

### **8.1 Slope Stability**

Slope stability results for the Pit 1 walls generally indicate adequate global stability for both static and pseudo-static conditions. Sections along the western highwall had the lowest factors of safety due to greater slope angles and wall heights.

The weak Mancos shale layer and estimated 45 ft surficial blast damage zone was found to be controlling factors in the computed failure surfaces. Anisotropic behavior of the Mancos shale does not indicate that bedding surfaces cause any significant change in stability.

FOS for surficial slope stability generally indicate adequate stability. The stability model does not capture any loose or eroded zones along the outermost surface of the highwall. Surficial failures not captured by modeling could still be possible along the outer highwall slopes but would be much smaller in scale. Removal of these loose materials is recommended.

Stability was analyzed for the current highwall slopes and pit floor elevations. Global stability would not be impacted by placement of fill in the pit bottom or scaling of surficial materials from the walls.

### **8.2 Rockfall Hazards**

Rockfall model results indicate that the west highwall presents the greatest rockfall hazard, predominantly originating from Dakota and Mancos formation seeder locations, requiring mitigation methods as part of the closure plan. Although rockfall was observed at sections RF-1 through RF-3 and RF-8, the overall runout, bounce heights, geometry, and pit floor elevation in these locations indicate the hazard is significantly lower than the sections along the west highwall. Sections RF-1 and RF-3 indicate greater than 99% of the modeled rockfall remains less than 25 ft from the toe of the slope in these areas. Typical operational controls at open pit mines prohibit workers from working within this distance of a highwall. Sections RF-2 and RF-8 have rockfall with a considerable amount of energy running out from the toe, however the majority of the rockfall remains inside of the edge of the haul roads that pass through these areas.

Sections RF-4 through RF-8 suggest that runout distance generally increases towards the south end of the west highwall, along with the amount of energy of the rockfalls. These sections have a higher percentage of modeled rockfall running out past 50 ft in the existing slope state, which is mostly a result of talus slopes promoting greater bounce / roll distances. Improvements to the pit floor will reduce this, but not enough to reduce the hazard significantly. Mitigation measures to reduce risk during construction under the closure plan and to reduce long term risks along the west highwall will be evaluated in the 90% CCOP.



Rockfalls modeled for Pit 1 generally focus on Dakota and Mancos formation hazards as these are the predominant rock types observable at the site as existing hazards and having previously fallen into the pit at the time of this analysis.

### **8.3 Recommended Next Steps**

Slope stability results met the minimum comparison FOS and would not require large scale slope changes.

The following recommendations are primarily for rockfall hazard mitigation. The 30% closure plan includes upstream drainage channels to divert water around the top of the highwall which is anticipated reduce weathering and erosion. However, flowing water is not the only weathering mechanism at this site.

We recommend the following actions and mitigation strategies.

- Incorporating rockfall modelling into the design analysis to confirm the appropriate sizing required for potential mitigation options such as rockfilled barriers, ditches, berms, or a combination of these options.
- Scaling (removal of loose-hanging eroded rock blocks) and debris removal along the pit crest, mid-slope benches, and the toe of the slope to decrease the immediate rockfall hazards prior to large scale earthwork in the pit bottom.
- Rockfall signage and specific guidance on setback distance to be maintained during O&M activities should be implemented for both construction and closure. Additional design details will be provided in the 90% CCOP.



## **9.0 REFERENCES**

- Abramson, L.W., Lee, T.S., Sharma, S. and Boyce, G.M. (2001). Slope Stability and Stabilization Methods, 2nd edition, John Wiley & Sons.
- Ashayer, Parham. (2007). Application of Rigid Body Impact Mechanics and Discrete Element Modeling to Rockfall Simulation. University of Toronto, Graduate Department of Civil Engineering – Ph.D. Thesis.
- Barton, N. and Choubey, V. (1977) The Shear Strength of Rock and Rock Joints in Theory and Practice. *Rock Mechanics*, 10, 1-54.
- Bieniawski, Z.T. (1989). *Engineering Rock Mass Classifications*. Wiley-Interscience, New York.
- Global Industry Standard on Tailings Management (GISTM). (2020).  
<https://globaltailingsreview.org>
- Hencher, S.R. (1995). Interpretation of direct shear tests on rock joints. *Rock Mechanics*, Balkema, Rotterdam.
- Hoek, E., Carter, T.G., Diederichs, M.S. (2013). Quantification of the Geological Strength Index Chart. ARMA 47th US Rock Mechanics/Geomechanics Symposium, San Francisco, CA, USA, 672-679.
- Hoek, E. and Brown, E.T. (2019). The Hoek-Brown failure criterion and GSI – 2018 edition. *Journal of Rock Mechanics and Geotechnical Engineering* 11 (2019), pp 445-463.
- INTERA Incorporated (INTERA), 2015. *St. Anthony Mine Stage 2 Abatement Plan – Cibola County, New Mexico*. February 9 (Modified).
- International Society for Rock Mechanics (ISRM) (2007). The complete ISRM suggested methods for rock characterization, testing and monitoring. Ulusay, R. and Hudson, J.A. (Eds.). Ankara, Turkey.
- Marinos, P., Marinos, V. and Hoek, E. (2007). The geological strength index (GSI): A characterization tool for assessing engineering properties for rock masses.
- Marinos, P. and Hoek, E. (2000). Estimating the mechanical properties of heterogeneous rock masses such as flysh.
- Read, J. and Stacey, P. (2019). *Guidelines for Open Pit Slope Design*. CSIRO Publishing, Australia.



**St. Anthony Mine: Pit 1 Highwall Stability – Phase 2 Report**  
**9.0 References**

Stantec Consulting Services, Inc. (Stantec). 2022. St Anthony Mine Site Closure Closeout Plan (CCOP) 30% Design Report. October 7.

Wyllie, D.C. (2018). Rock Slope Engineering, Civil Applications. 5th Edition, CRC Press.

Wyllie, D.C. (2015). Rock Fall Engineering., CRC Press.



**APPENDIX A      PHASE 2 WORKPLAN**



**APPENDIX B      SITE PLAN**



**APPENDIX C      BOREHOLE LOGS**



## APPENDIX D      PHOTOLOGS



## APPENDIX E DATA VISUALIZATION



**APPENDIX F TELEVIEWER LOGS**



## APPENDIX G      DILATOMETER RESULTS



## APPENDIX H      RADIATION SCAN DATA



**APPENDIX I      LAB TEST RESULTS**



**APPENDIX J      GSI**



## APPENDIX K      KINEMATIC RESULTS



**APPENDIX L      SLOPE STABILITY RESULTS**



**APPENDIX M    ROCKFALL RESULTS**

